1 Structural imaging of native cryo-preserved secondary cell walls

2 reveals presence of macrofibrils composed of cellulose, lignin and

3 xylan.

- 4 Jan J. Lyczakowski^{1,2}, Matthieu Bourdon³, Oliver M. Terrett¹, Ykä Helariutta^{3,4},
- 5 Raymond Wightman^{3,#} and Paul Dupree^{1,2,#}
- 6
- ⁷ ¹ Department of Biochemistry, University of Cambridge, Tennis Court Road,
- 8 Cambridge, CB2 1QW, UK
- ⁹ ² Natural Material Innovation Centre, University of Cambridge, 1 Scroope Terrace,
- 10 Cambridge, CB2 1PX, UK
- ³ The Sainsbury Laboratory, University of Cambridge, Bateman Street, Cambridge,
- 12 CB2 1LR, UK
- ⁴ Institute of Biotechnology/Department of Biological and Environmental Sciences,
- 14 University of Helsinki, FIN-00014, Finland
- 15
- ¹⁶ [#]Address correspondence to Raymond Wightman
- 17 (<u>raymond.wightman@slcu.cam.ac.uk</u>) or Paul Dupree (<u>pd101@cam.ac.uk</u>).
- 18
- 19
- 20
- 21
- ---
- 22
- 23
- 24
- 25
- -
- 26

27 Abstract:

28 The woody secondary cell walls of plants are the largest repository of renewable carbon biopolymers on the planet. These walls are made principally from cellulose and 29 hemicelluloses and are impregnated with lignin. Despite their importance as the main 30 load bearing structure for plant growth, as well as their industrial importance as both a 31 material and energy source, the precise arrangement of these constituents within the 32 cell wall is not yet fully understood. We have adapted low temperature scanning 33 electron microscopy (cryo-SEM) for imaging the nanoscale architecture of angiosperm 34 35 and gymnosperm cell walls in their native hydrated state. Our work confirms that cell wall macrofibrils, cylindrical structures with a diameter exceeding 10 nm, are a 36 37 common feature of the native hardwood and softwood samples. We have observed these same structures in Arabidopsis thaliana secondary cell walls, enabling 38 macrofibrils to be compared between mutant lines that are perturbed in cellulose, 39 40 hemicellulose and lignin formation. Our analysis indicates that the macrofibrils in Arabidopsis cell walls are composed, at least partially, of cellulose, xylan and lignin. 41 42 This study is a useful additional approach for investigating the native nanoscale architecture and composition of hardwood and softwood secondary cell walls and 43 demonstrates the applicability of Arabidopsis genetic resources to relate fibril structure 44 with wall composition and biosynthesis. 45

Keywords: SEM, cell walls, macrofibrils, cellulose, xylan, lignin, softwood, hardwood,

47 Arabidopsis thaliana

48

49 Introduction:

The majority of carbon in terrestrial biomass is stored in forests as wood (Ramage et 50 al., 2017, Pan et al., 2011). The current classification system distinguishes two types 51 of timber. Wood from Angiosperm trees is known as hardwood and the wood made by 52 Gymnosperm species is described as softwood (Ramage et al., 2017). Despite 53 significant differences in tissue organisation and chemical composition, both these 54 types of timber are almost entirely formed from plant secondary cell walls - an 55 extracellular matrix made primarily from cellulose, lignin and hemicelluloses 56 (Schweingruber, 2007). Considering the ecological and industrial importance of wood 57 and other cell wall materials, our knowledge of the exact arrangement of these 58 polymers in the cell wall remains poor. A better understanding of the molecular 59

architecture and ultrastructure of cell walls is needed to describe the complex
spatiotemporal deposition pattern of the cell wall polymers. This may contribute to the
development of more efficient biofuel feedstocks (Loque et al., 2015), to the
improvement in our understanding of novel biomaterials such as nanocellulose (Jarvis,
2018), and to applications such as advanced approaches for the use of timber in the
construction industry (Ramage et al., 2017)

Cellulose is the main constituent of plant cell walls (Pauly and Keegstra, 2008). At the 66 molecular level, cellulose has a simple repeating structure of β -1,4-linked 67 glucopyranosyl residues. These glucan chains coalesce to form a crystalline cellulose 68 microfibril. The exact structure of the microfibril is unknown, however, it has been 69 suggested the elementary microfibril consists of 18 or 24 individual glucan chains 70 (Gonneau et al., 2014, Hill et al., 2014, Turner and Kumar, 2017). Individual cellulose 71 microfibrils associate to form larger order structures known as macrofibrils (Niklas, 72 2004). In plant primary cell walls this close-contact association may be limited to 73 selected parts of microfibril which is proposed to lead to formation of so-called 74 biomechanical hotspots (Cosgrove, 2014). A range of imaging and spectroscopic 75 techniques has been used to investigate cellulose macrofibrils in secondary cell walls, 76 as reviewed by (Purbasha et al., 2009), but due to technical challenges the precise 77 structure in native, unprocessed, hydrated secondary cell walls remains poorly 78 described. Lignin is the main non-polysaccharide component of both hardwood and 79 softwood and is made by coupling of monolignol radicals in secondary cell walls. Three 80 main monolignols exist in plants, which, once turned into chemical radicals by the 81 activity of laccases and peroxidases, can couple in a random manner to form a lignin 82 polymer made from guaiacyl (G), syringyl (S), and p-hydroxyphenyl (H) units (Ralph et 83 al., 2004). The monolignol composition of hardwood and softwood differs, with the 84 former consisting of predominantly S and G units and the latter being made almost 85 solely from G units (Vanholme et al., 2010). The process of lignification is important 86 for wood mechanical properties. Arabidopsis mutant plants with reduced lignin content 87 or altered monolignol composition often have collapsed xylem vessels and can be 88 severely dwarfed (Bonawitz and Chapple, 2010). Lignin is proposed to associate with 89 cell wall polysaccharides to form the recalcitrant matrix (Terrett and Dupree, 2019). 90

Xylan and galactoglucomannan are the principal hemicelluloses in hardwood and 91 softwood. Xylan is a polymer of β -1,4-linked xylopyranosyl residues and is the main 92 hemicellulose in hardwood but is also present in softwood (Scheller and Ulvskov, 93 2010). Hardwood and softwood xylans carry α -1–2 linked glucuronic acid (GlcA) 94 branches which can be methylated on carbon 4 leading to formation of 4-O-95 Methylglucuronic acid (MeGlcA) (Scheller and Ulvskov, 2010). In addition to GlcA and 96 Me GlcA (together, [Me]GlcA) decorations, hardwood xylan hydroxyls are acetylated 97 98 on carbon 2, carbon 3 or both carbons of the monomer. The softwood xylan, in addition to the MeGlcA branches, carries α -1,3–linked arabinofuranosyl decorations (Scheller 99 and Ulvskov, 2010, Busse-Wicher et al., 2016b). The presence of [Me]GlcA branches 100 on xylan is important for the maintenance of biomass recalcitrance (Lyczakowski et 101 al., 2017) and, together with acetylation in hardwood and arabinose decorations in 102 softwood, these substitutions are mostly distributed with an even pattern on xylosyl 103 units (Bromley et al., 2013, Busse-Wicher et al., 2014, Busse-Wicher et al., 2016b, 104 Martinez-Abad et al., 2017). This so-called 'compatible' patterning of xylan 105 substitutions is thought to allow the hydrogen bonding between xylan, in a two-fold 106 107 screw conformation, and the hydrophilic surface of the cellulose microfibril (BusseWicher et al., 2016a, Simmons et al., 2016, Grantham et al., 2017). 108 109 Galactoglucomannan (GGM) is the main hemicellulose in softwood (Scheller and 110 Ulvskov, 2010) but is also present in hardwood xylem. GGM has a backbone formed from both β -1,4-linked mannosyl and glucosyl residues with some mannosyl residues 111 substituted by an α-1,6-linked galactosyl branch. The GGM backbone can also be 112 acetylated. The arrangement of mannose and glucose units in softwood GGM is 113 thought to be random, but a recently described regular structure GGM found in 114 Arabidopsis mucilage was proposed to bind to both the hydrophilic and hydrophobic 115 surface of the cellulose microfibril (Yu et al., 2018). In vitro studies using TEM and 1D 116 ¹³C NMR indicate that a range of branched and unbranched mannan and glucomannan 117 structures can interact with bacterial cellulose (Whitney et al., 1998). Softwood GGM 118 is also proposed to interact with the cellulose microfibril (Terashima et al., 2009) and 119 recent evidence demonstrates that it can form covalent linkages with lignin (Nishimura 120 121 et al., 2018).

122 Although we now have a better understanding of secondary cell wall composition and 123 the nature of the interactions between its main constituents, a picture of the

ultrastructural assembly of wall polymers into a secondary cell wall matrix is not yet 124 complete. Solid state NMR (ssNMR) analysis has been applied extensively to the 125 study of polymer interactions in both primary and secondary walls. This, for example, 126 provided evidence that in dried primary wall samples from Arabidopsis, pectin and 127 xyloglucan may be interacting with the cellulose microfibril (Dick-Perez et al., 2011). 128 Analysis of hydrated secondary cell wall of Arabidopsis with solid state NMR indicated 129 that xylan is likely to interact with the hydrophilic surface of the cellulose microfibril as 130 a two-fold screw (Simmons et al., 2016, Grantham et al., 2017). Recent ssNMR 131 analysis indicates that in dried cell walls of grasses xylan is likely to interact with lignin 132 (Kang et al., 2019). Despite providing excellent insights into the proximity of different 133 cell wall components ssNMR cannot provide information about the assembly of these 134 constituents into higher order structures. Some insights into this process have been 135 other techniques. This includes application of vibrational 136 achieved with microspectroscopy techniques such as FT-IR and RAMAN to study the orientation of 137 cellulose and other cell wall components in the matrix, as reviewed by (Gierlinger, 138 2018). AFM has been applied to the study of cell wall matrix assembly, but the work 139 140 has been focused on primary cell walls (Cosgrove, 2014) and only recent advances allowed nanoscale resolution imaging of dried spruce secondary cell walls (Casdorff 141 142 et al., 2017). Moreover, insights into the assembly of cellulose microfibrils in wood 143 walls of conifers (Fernandes et al., 2011) and dicots (Thomas et al., 2014) have been obtained using wide-angle X-ray scattering (WAXS) and small-angle neutron 144 scattering (SANS). 145

In addition to these various approaches, other studies have attempted to use scanning 146 electron microscopy (SEM) to study the structure of plant cell walls. Low temperature 147 SEM (cryo-SEM), in which the sample is rapidly frozen and then maintained cold 148 during imaging, has been used to study the collapse of pine needle tracheid cell walls 149 upon prior dehydration (Cochard et al., 2004) and to visualise the bulging of root hairs 150 in the *kojak* (cellulose synthase-like) mutant (Favery et al., 2001). Additionally, higher 151 magnification cryo-SEM has been used to visualise cell walls of wheat awns (Elbaum 152 et al., 2008). Some awn cell walls exhibit structural differences that are dependent 153 upon the level of hydration and cryo-SEM revealed extensive layering within the wall, 154 however, the technique was not further optimised to investigate individual fibrils. Field 155 emission (FE) SEM techniques were effectively used to study the alignment of 156

cellulose microfibrils in Arabidopsis hypocotyls (Refregier et al., 2004), roots 157 (Himmelspach et al., 2003) and stems (Fujita et al., 2013). FE-SEM has also been 158 applied to investigate wood structure, including observations of microfibril alignment in 159 fixed cell walls of fir tracheids (Abe et al., 1997) and lignin distribution in spruce 160 tracheids (Fromm et al., 2003). Importantly, FE-SEM analysis of dehydrated pine and 161 poplar wood suggests that secondary cell walls of these species contain macrofibrils 162 - cylindrical fibrillar structures with a diameter of up to 60 nm, which presumably 163 164 comprise of bundles of elementary cellulose microfibrils (Donaldson, 2007). Moreover, the diameter of these macrofibrils was observed to increase with increasing 165 lignification, suggesting that the macrofibrils may be formed from association of lignin 166 and cell wall polysaccharides. This analysis was extended further to wood from Ginkgo 167 where the FE-SEM was combined with density analysis to propose a model of 168 macrofibril formation based on cellulose, GGM, xylan and lignin interaction (Terashima 169 et al., 2009). 170

It has been suggested that some of the treatments used in preparation of the FE-SEM 171 cell wall samples have little impact on the microfibril alignment and that the technique 172 173 may provide a true representation of native (unprocessed) cell wall features (Marga et al., 2005). The FE-SEM techniques applied to secondary cell wall samples, however, 174 included additional steps such as (i) fixation and exposure to organic solvents (ii) a 175 thermal treatment that may result in some degree of wall degradation (Fromm et al., 176 2003) and (iii) a thick coating of heavy metal which may impact upon the resolution 177 (Donaldson, 2007), raising questions about the effect these may have on interpretation 178 of the wall structure. Visualisation of native, hydrated, secondary cell walls with 179 environmental FE-SEM has been challenging and the resolution of obtained images 180 has been low (Donaldson, 2007). We present here a technique for the analysis of 181 native, fully-hydrated, secondary cell wall material from angiosperm and gymnosperm 182 plant species using cryo-SEM. The use of an ultrathin 3 nm platinum film, together with 183 cryo-preservation at high vacuum, enabled us to demonstrate that cell wall macrofibrils 184 are a common feature in all types of native secondary cell wall material analysed. 185 Importantly, we were able to detect the presence of macrofibrils in Arabidopsis thaliana 186 vessel secondary cell walls. This allowed us to make use of the readily available cell 187 wall-related genetic resources, revealing Arabidopsis macrofibril diameter to be 188 189 dependent upon cellulose, xylan and lignin.

190

191 **Results:**

192 Softwood and hardwood secondary cell walls contain macrofibrils

In order to investigate and compare the nanoscale architecture of gymnosperm and 193 angiosperm cell walls we analysed stem sections taken from spruce, Ginkgo and 194 poplar using cryo-SEM. Stems were placed in the SEM specimen stub and 195 immediately frozen in nitrogen slush, fractured and then coated with platinum, before 196 being passed in to the SEM chamber for imaging. Nitrogen slush is a suspension of 197 solid nitrogen that enables high freezing rates, greatly reducing the Leidenfrost effect 198 during plunge freezing and thus minimising structural damage (Sansinena et al., 199 200 2012). The fine grain size attributed to platinum sputtering allows small and densely packed objects to be resolved. This rapid sample preparation protocol serves to better 201 maintain sample hydration levels and native structures for optimal EM imaging in a 202 high vacuum environment. 203

We first investigated whether our cryo-SEM protocol gave comparable results to the 204 previous FE-SEM analysis of both softwood and hardwood secondary cell walls 205 206 (Donaldson, 2007). To examine if macrofibrils are found in natively hydrated, nonpretreated cell walls, cryo-SEM imaging was performed on unprocessed, frozen 207 208 softwood and hardwood samples. For observing gymnosperm cell wall architecture, we first prepared softwood samples from spruce and used a low magnification to see 209 an overview of stem cross-section (Figure 1a) and tracheid structure (Figure 1b). The 210 inner part of the stem cross section was composed of densely packed xylem tracheids, 211 each surrounded by cell walls. To investigate the appearance of the secondary cell 212 walls, higher magnification images of these parts of tracheid cells were acquired. This 213 enabled us to observe that the tracheid cell walls contain fibrous structures which 214 frequently assembled into larger aggregates (Figure 1c and 1d, red arrows). After a 215 further increase in magnification, individual fibrils became resolvable (Figure 1e and 216 1f) and their diameter was found to exceed the 3 nm diameter calculated for a single 217 218 softwood elementary microfibril (Fernandes et al., 2011). Therefore the observed fibrils, if composed of cellulose, represent a higher order structure that fits the 219 description of a "macrofibril" (Niklas, 2004, Donaldson, 2007). Similarly to spruce stem, 220 sections from another gymnosperm, the Ginkgo, were also observed to contain 221

macrofibrils (Figure S3). These data show that, in line with previously reported SEM
imaging of dried, processed plant material (Donaldson, 2007, Terashima et al., 2009),
the native, hydrated cell walls of spruce and Ginkgo also contain macrofibrils.
Therefore, these structures may contribute to the higher order assembly of native
gymnosperm cell walls.

227 We extended the analysis to the model hardwood species, poplar. Vessels, a distinct cell type of hardwood xylem, were clearly visible using low magnification (Figure 2a 228 and 2b). In addition to the vessels, xylem fibre cells were also observed (Figure 2b; 229 red and yellow arrows for vessels and fibre cells respectively). For some cells we were 230 able to observe spiral thickenings which were preserved during sample preparation 231 and extended above the surface of the fracture plane (Figure 2b). We focused upon 232 the vessel cell walls which showed clearly visible fibrous structures at a vessel-233 tovessel boundary (Figure 2c). Analysis of vessel cell walls at a higher magnification 234 revealed a clear presence of macrofibril structures, similar to those observed in spruce, 235 236 in the poplar samples (Figure 2d and 2e). To investigate the dimensions of the macrofibrils we measured their diameter in poplar and spruce (Figure 2f). Our 237 238 measurements are broadly similar to those reported in a previous study (Donaldson, 2007). We carried out comparative analysis of macrofibril diameter between hardwood 239 and softwood by measuring 150 individual macrofibrils in poplar, spruce and Ginkgo. 240 While the diameter of spruce and Ginkgo macrofibrils was not significantly different 241 (Figure S4), the diameter of macrofibrils in poplar secondary cell walls was significantly 242 smaller than that of spruce macrofibrils (Figure 2f). Spruce and Ginkgo were grown in 243 the field while poplar samples were obtained from in vitro grown plants. To control for 244 this difference in growth conditions we also analysed samples from field grown poplar 245 trees. There was no statistically significant difference in the macrofibril diameter 246 between the two poplar samples (Figure S5). For both hardwood and softwood we 247 observed variation in the macrofibril diameter. This may reflect biological differences 248 or may be a result of technical challenges associated with macrofibril width 249 250 measurement.

251 Arabidopsis secondary cell walls macrofibrils contain a cellulose scaffold

To further evaluate the nanoscale architecture of plant cell walls and identify possible constituents of the cell wall macrofibrils, the high magnification cryo-SEM imaging was

used to analyse wild type (WT) Arabidopsis secondary cell walls (Figure 3). The initial 254 analysis investigated the structure of WT xylem vessels (Figure 3a and 3b). Sets of 255 vessel bundles were detected and, using higher magnification, fibrous structures 256 similar to those observed in spruce and poplar were also visible in the fractured 257 Arabidopsis material. The width of WT Arabidopsis macrofibrils was comparable to 258 that of poplar macrofibrils but not spruce and suggests Arabidopsis macrofibrils could 259 be used as a good structural model for hardwoods (Figure S4, S5). Despite the use of 260 261 ultra-thin platinum coating, the use of SEM without the cryo-preservation steps did not allow us to observe the Arabidopsis macrofibrils with good resolution (Figure S6) 262 highlighting the critical importance of sample cryo-preservation to resolve a native cell 263 wall ultrastructure. 264

Based on the data available in the literature we hypothesized that the macrofibrils may 265 be mostly composed of cellulose (Fahlen and Salmen, 2002, Donaldson, 2007). To 266 investigate this, and to understand the nature of these macrofibrils further, we 267 268 performed a comparative analysis between WT vessel cell walls (Figure 3c) and a commercially available fibrous cellulose standard (Figure 3d) extracted from cotton 269 270 linters and consisting of 99% pure cellulose (Sczostak, 2009). In this experiment, clear individual fibrils with distinct bright termini were observed in both samples indicating 271 that the vessel wall macrofibrils have a similar appearance to the cellulose fibrils 272 present in this polysaccharide standard. To determine whether these macrofibrils are 273 dependent upon the proper production of cellulose, the morphology of WT Arabidopsis 274 vessel cell walls (Figure 3e and 3g) was compared to that of the *irx*3 mutant (Figure 3f 275 and 3h). IRX3 is one of three CESA proteins that make up the secondary wall cellulose 276 synthase complex and *irx3* plants are almost completely devoid of cellulose in their 277 secondary cell walls, but not primary cell walls (Taylor et al., 1999). As previously 278 279 reported, *irx3* plants had collapsed vessels (Figure S7), since secondary cell wall cellulose contributes to vessel wall strength (Turner & Somerville, 1997). Interestingly, 280 the *irx3* stems lacked the fibrous structures in their vessel secondary cell walls and, in 281 contrast to WT, the *irx*3 cell walls were formed from a largely amorphous matrix (Figure 282 3f). It is likely that this matrix is composed of xylan and lignin, which can still be 283 deposited in the secondary cell wall in the absence of IRX3 activity (Takenaka et al., 284 2018). Some structures resembling the macrofibrils were present in the primary cell 285

walls of *irx3* plants (Figure S7). Taken together, the data demonstrate macrofibril
 formation is dependent upon cellulose production.

Reduction in cell wall xylan and lignin, but not in galactoglucomannan content decreases the dimensions of Arabidopsis macrofibrils

To investigate the role of xylan in macrofibril formation, cryo-SEM was used to 290 visualise the secondary walls from *irx9*, *irx10* and *esk1* Arabidopsis plants (Figure 4a, 291 4b and 4c). IRX9 and IRX10 are required for proper xylan synthesis and mutations in 292 the corresponding genes lead to cell wall weakening and collapse of xylem vessels in 293 the Arabidopsis model (Brown et al., 2007, Bauer et al., 2006, Brown et al., 2005). The 294 *irx9* plants have impaired xylan synthesis resulting in a decrease of xylan by more than 295 50% compared to WT (Brown et al., 2007). In *irx10* plants the reduction in xylan 296 content is smaller and does not exceed 20% (Brown et al., 2005). Macrofibrils are 297 clearly observed in *irx9* and *irx10* Arabidopsis (Figure 4a and 4b). However, the 298 299 median macrofibril diameter between WT and *irx9* cell wall fibres showed a ~30% reduction in the xylan synthesis mutant (Figure 4g). The median macrofibril diameter 300 of *irx10* plants was ~10% smaller than that of WT Arabidopsis (Figure 4g). Although 301 there was a wide variation in macrofibril diameter within each genotype, the difference 302 between the WT macrofibril diameter and the one quantified for the two mutants is 303 statistically significant, suggesting that xylan is incorporated along with cellulose to 304 generate the normal macrofibril size. To investigate the role of xylan-cellulose 305 interaction in the macrofibril formation we assessed the macrofibril size in the esk1 306 Arabidopsis mutant (Figure 4c). Mutation in the ESK1 gene results in reduction of xylan 307 acetylation, but not in a decrease in xylan quantity (Xiong et al., 2013), which leads to 308 309 changes in xylan [Me]GlcA patterning and loss of interaction between xylan and the hydrophilic surface of the cellulose microfibril (Grantham et al., 2017). In line with the 310 results observed for *irx9* and *irx10* plants the loss of xylan-cellulose interaction caused 311 a reduction in the macrofibril diameter (Figure 4g). 312

Previous work in softwood suggested that lignin (Donaldson, 2007) and galactoglucomannan (GGM) (Terashima et al., 2009) may be involved in macrofibril formation. To investigate the role of these two cell wall components in the maintenance of macrofibril structure we performed imaging of *4cl1* (Figure 4d), *lac4* (Figure 4e) and *csla2/3/9* (Figure 4f) mutant Arabidopsis cell walls. Both 4CL1 and LAC4 are involved

in lignin biosynthesis and plants mutated in genes encoding these enzymes have a 318 30% and 15% reduction in lignin content respectively (Li et al., 2015, Berthet et al., 319 2011). The median macrofibril diameter for both 4cl1 and lac4 was significantly smaller 320 than that calculated for WT (Figure 4g). Importantly, the extent of the reduction in 321 macrofibril diameter was in line with the decrease in the lignin content observed for the 322 two mutants, with 4cl1 macrofibrils being ~15% smaller than the WT ones and lac4 323 macrofibrils having ~7% reduction in the median diameter. Proteins from the CSLA 324 family are involved in the biosynthesis of a hemicellulose galactoglucomannan and 325 mutations in csla2/3/9 leads to nearly complete loss of stem GGM in the Arabidopsis 326 model (Goubet et al., 2009). Our quantitative analysis indicates that the diameter of 327 macrofibrils of cs/a2/3/9 Arabidopsis was not significantly different to that of the WT 328 plants (Figure 4g). 329

330

331 Discussion

The native nanoscale architecture of woody plant secondary cell walls remains poorly 332 understood due to the challenges of keeping the sample hydrated, which is 333 incompatible with some types of techniques. Studies analysing dehydrated and fixed 334 plant cell wall samples with FE-SEM (Donaldson, 2007), together with other work 335 which includes SANS experiments investigating spruce (Fernandes et al., 2011) and 336 bamboo samples (Thomas et al., 2015), suggest there is a higher order arrangement 337 of cellulose microfibrils in plant secondary cell walls. Our work reports the application 338 of a cryo-SEM based analysis technique which, using exclusively samples that have 339 not been dried, heated or chemically processed, indicates that secondary cell wall 340 cellulose microfibrils are likely to come together to form larger macrofibril structures. 341

Our study strongly suggests that these structures, at least in the model plant species *Arabidopsis thaliana,* contain cellulose, xylan and lignin.

Previous studies investigated the presence and diameter of macrofibrils in dehydrated softwood samples (Donaldson, 2007). In line with results presented in our work, Donaldson did observe macrofibrils in cell walls of pine tracheids. Moreover, also in agreement with the results presented here (Figure S4), these softwood macrofibrils were larger than those seen in hardwoods. In softwood, in addition to various patterned

types of xylan (Busse-Wicher et al., 2016b, Martinez-Abad et al., 2017), most of which 349 are likely to be compatible with binding to the hydrophilic surface of the cellulose fibril, 350 the cell walls contain large quantities of acetylated GGM (Scheller and Ulvskov, 2010) 351 which may contribute to macrofibril width. Indeed, gymnosperm GGM was proposed 352 to interact with the cellulose microfibril in cell walls of Ginkgo (Terashima et al., 2009). 353 Therefore, the significant difference in macrofibril diameter observed between 354 hardwood and softwood samples may be due to the differences in the cell wall 355 356 composition. Consequently, we hypothesize that in gymnosperms, GGM, along with xylan, may contribute to the macrofibril size in a way similar to what we observed for 357 xylan in Arabidopsis macrofibrils. With an average diameter ranging between 20 and 358 34 nm, the size of pine macrofibrils measured by Donaldson was somewhat smaller 359 than that measured in spruce wood in the current work. However, these observations 360 are not necessarily inconsistent. Donaldson dehydrated the wood samples prior to the 361 SEM imaging. As the spacing between bundled softwood cellulose microfibrils, 362 363 estimated to be equal to 3 nm by small angle neutron scattering, is sensitive to wood hydration levels (Fernandes et al., 2011), at least part of the difference in the 364 365 macrofibril diameter might be due to the changes in the water content within the sample analysed with SEM. Interestingly, Donaldson reported that macrofibrils in dried 366 poplar wood, depending on their position in cell wall, have an average diameter 367 368 ranging from 14 to 18 nm, which is similar to what was measured for both poplar and Arabidopsis as a part of our study. This observation suggests that the softwood 369 macrofibril size may be more sensitive to drying than the hardwood one. This in turn 370 suggests that, in addition to compositional disparities, hydration could contribute to the 371 372 differences in softwood and hardwood macrofibril characteristics. In addition to providing scientific insight, this result highlights that imaging of the cryopreserved 373 374 secondary cell walls offers significant advance over the previously used techniques.

Interestingly, similar to a previous report (Donaldson, 2007), we observed that macrofibrils in both hardwood and softwood have a range of diameters. The reasons for this variation in size are not clear. It is possible that the number of individual cellulose microfibrils that come together to form the macrofibril structure in both hardwood and softwood is not constant. This may be regulated by coordinated movement of CesA complexes or their density during cell wall synthesis (Li et al., 2016). It was proposed that the macrofibril diameter is proportional to the degree of

cell wall lignification (Donaldson, 2007), which may also vary between the structures. 382 This hypothesis is supported by our results which indicate that the cell wall lignin 383 content influences macrofibril diameter in Arabidopsis. Variations may also originate 384 from environmental conditions. For example, it was shown that wood density may vary 385 correlatively with climate change (Bouriaud et al., 2005). Although much of this effect 386 is likely to be due to cell size and wall thickness, it can be hypothesized that change 387 in wood density may also originate from compositional changes that impact macrofibril 388 389 assembly and ultrastructure. It would therefore be relevant to assess macrofibrils of perennial trees with samples spanning several years of growth. We cannot rule out 390 that the width variance may originate from the technical limitations of resolving the 391 macrofibrils by SEM. It will be interesting to see if the emerging He-ion technologies, 392 with an increase in resolution and less dependent upon metal coating, reduce this 393 variance (Joens et al., 2013). The cryo-SEM techniques developed as part of our study 394 offer a significant advantage over the previous investigation (Donaldson, 2007) which 395 396 applied a thicker coat of chromium (mostly 12 nm) that yield films with coarser grains than the thinner (3 nm) platinum films used in our work. Thus, taking the results 397 398 described by Donaldson and our technological improvements into consideration, we believe that the variance in the macrofibril width observed in both studies is likely to 399 400 reflect natural material variation.

The prominence of macrofibril structures in Arabidopsis cell walls is a surprising 401 discovery of this study. Previously published results using AFM analysis indicate the 402 403 presence of some bundled microfibrils in primary cell walls of Arabidopsis but the extent of this bundling is lower than what was observed in primary cell wall samples 404 405 from other species (Zhang et al., 2016). AFM is not yet technically feasible for analysis of bundling of hydrated secondary cell walls although recent technical advances 406 allowed visualisation of dried spruce wood at a nanometer resolution (Casdorff et al., 407 2017). The observation of the macrofibrils by cryo-SEM in Arabidopsis allowed us to 408 determine the contribution of cellulose, xylan, lignin and galactoglucomannan to 409 macrofibril formation, thanks to the availability of secondary cell wall related mutants 410 in this model. Macrofibrils were completely absent in vessel cell walls of *irx3* plants, 411 which lack secondary cell wall cellulose, indicating that proper cellulose biosynthesis 412 is required for formation and assembly of secondary cell walls polymers into 413 414 macrofibrils. In addition, we observed that vessel macrofibril diameter is significantly

decreased in *irx9, irx10* and *esk1* plants, suggesting that xylan may also participate in 415 the correct assembly of such structures. While in *irx9* and *irx10* reduction in macrofibril 416 diameter may be associated with decrease in the xylan content the ~25% reduction in 417 the median macrofibril diameter observed for esk1 Arabidopsis is harder to explain. 418 Hardwood xylan is proposed to interact with the hydrophilic surface of the cellulose 419 microfibril as a two-fold screw (Simmons et al., 2016, Busse-Wicher et al., 2016a), and 420 this interaction is facilitated by the even pattern of the [Me]GlcA and acetyl branches 421 422 on the xylan backbone which is lost in *esk1* plants (Grantham et al., 2017). Therefore, the decrease in macrofibril diameter observed in esk1 Arabidopsis indicates that 423 xylancellulose interaction may have a role in spacing or proper coalescence of 424 microfibrils to form the elementary macrofibril. It is unclear why the macrofibril diameter 425 is reduced in *esk1*, but perhaps fewer elementary fibrils are incorporated into each 426 macrofibril when xylan is not interacting with the hydrophilic surface of the cellulose 427 fibril. This may be different to the effect observed in flax where the absence of xylan 428 may lead to aggregation of glucan chains into larger fibres (Thomas et al., 2013). Such 429 difference may be associated with variations in the stoichiometry of the cellulose 430 431 synthase complex which were recently reported for angiosperms (Zhang et al., 2018).

In addition to implicating xylan in the process of macrofibril formation our results 432 indicate that lignin may contribute to assembly of the structures. As such, our results 433 use genetic assignment to extend previous work which has correlated macrofibril 434 diameter with the degree of wall lignification (Donaldson, 2007). Interestingly, we 435 436 observed that the macrofibril diameter does not correlate with the cell wall GGM content. This may be associated with low abundance of GGM in angiosperms where 437 the polysaccharide accounts for only up to 5% of the cell wall material (Scheller and 438 Ulvskov, 2010). Alternatively, this result may indicate that in Arabidopsis GGM might 439 be not involved in macrofibril formation. GGM may play a more significant role in the 440 macrofibril assembly in gymnosperms where it accounts for up to 30% of the cell wall 441 material. Importantly, all our conclusions are based on the analysis of native, hydrated, 442 cell wall samples. The assignment of cell wall macrofibril composition, in their native 443 state, would be impossible using techniques such as immunogold due to the 444 pretreatment steps needed before the antibody labelling. 445

In conclusion, our analysis indicates that vessel cell walls contain fibrous structures 446 composed of cellulose, xylan and lignin. These structures are present in both 447 hardwood and softwood and have a diameter larger than a single cellulose microfibril. 448 Therefore, these structures can be described as cell wall macrofibrils. The reduction 449 in macrofibril diameter observed in *esk1* Arabidopsis suggests that the interaction 450 between xylan and the hydrophilic surface of the cellulose microfibril may be involved 451 in the assembly of these structures. Therefore, this xylan-cellulose interaction may be 452 453 important for the maintenance of plant cell wall ultrastructure and mechanical properties (Simmons et al., 2016). The techniques developed here and the discovery 454 of the ubiquitous presence of macrofibrils in hardwood and softwood in their native 455 state will contribute to a better understanding of cell wall assembly processes. 456 Furthermore, the ability to resolve macrofibrils in Arabidopsis, along with the 457 availability of genetic resources in this model, will offer the community a valuable tool 458 to further study the complex deposition of secondary cell walls polymers and their role 459 in defining the cell wall ultrastructure. The assembly of cell wall macrofibrils is likely to 460 influence the properties of wood, such as density, which may vary due to different 461 462 stimuli such as tree fertilisation (Makinen et al., 2002) or environmental changes (Bouriaud et al., 2005). Therefore, we expect that the methodology described here will 463 enable to correlate the native nanoscale features of the cell walls, such as the 464 465 macrofibril diameter, or a specific macrofibril patterning within the cell wall, with wood properties. Consequently, our approach may be useful to assess this aspect of wood 466 quality at a new level and could benefit numerous industries ranging from building 467 construction, paper manufacturing and biofuel production to generation of novel 468 469 biomaterials such as nanocrystalline cellulose.

470

471 Experimental procedures:

472 Plant material

Picea abies, (spruce) one-year old branch was acquired from 30-50cm tall potted
plants grown outdoors purchased from Scotsdale (Great Shelford, Cambridgeshire,
UK). *Ginkgo biloba,* (Ginkgo) stem material was obtained from the trees grown at the
Cambridge University Botanic Garden. For both spruce and Ginkgo, samples from two
individuals were analysed.

Hybrid aspen (*Populus tremula x Populus tremuloides*, clone T89), referred to as
poplar in the text, was grown *in vitro* (20°C, with a 16-h light, 8-h dark photoperiod,
with illumination at 85 microeinstein.m⁻².s⁻¹) during 76 to 80 days after
micropropagation on 1/2MS media with vitamins (Duchefa M0222), 1% sucrose, 0.7%
Agar. Samples from three individuals were analysed. For field grown poplar (*Populus tremula*), material was obtained from two individuals grown at the Cambridge
University Botanic Garden.

Arabidopsis thaliana (Arabidopsis) Columbia-0 ecotype plants were grown in a cabinet maintained at 21 °C, with a 16-h light, 8-h dark photoperiod. Stem material was collected from 7-week-old plants. Mutant insertion lines described in published work were used in this study. Specifically, *irx3-7* plants (Simmons et al., 2016, Kumar and Turner, 2015), representing a mutant allele of *CESA7*, *irx9-1* (Brown et al., 2005), *irx10-1* (Brown et al., 2005), *esk1-5* (Lefebvre et al., 2011, Grantham et al., 2017),

491 *4cl1-1* (Vanholme et al., 2012), *lac4-2* (Berthet et al., 2011) and *csla2-1csla3-2csla91*

492 (Goubet et al., 2009). Plants were analysed alongside the wild type (WT) material.

493 For each genotype three individuals were analysed.

494 Cryo-SEM sample preparation and imaging

Fresh stems of 7 week old Arabidopsis plants were prepared for imaging as outlined 495 in Supporting Information Figure S1. Firstly, 1 cm length sections were cut from the 496 bottom part of the stems and mounted vertically in recessed stubs containing a cryo 497 glue preparation consisting of a 3:1 mixture of Tissue-Tec (Scigen Scientific, USA) and 498 499 Aquadog colloidal graphite (Agar Scientific, Stansted, UK) (see steps 1 to 4 on Figure S1). Stem sections were immediately (within 5 minutes of harvest) plunge frozen in 500 liquid nitrogen slush (step 5 on Figure S1), transferred under vacuum, fractured and 501 then coated with 3 nm of platinum (step 6 on Figure S1) using a PT3010T cryo-502 apparatus fitted with a film thickness monitor (Quorum Technologies, Lewes, UK). The 503 short time between freezing and harvesting serves to prevent drying of the sample 504 where only the exposed surface, not the fractured face, is expected to exhibit some 505 water loss during the short time it is exposed to air. Finally, fractured stems were 506 imaged using a Zeiss EVO HD15 Scanning Electron Microscope (step 7 on Figure S1) 507 508 and maintained at -145 °C using a Quorum cryo-stage assembly. The electron source is a Lanthanum Hexaboride HD filament. Images were acquired using a secondary 509

electron detector and an accelerating voltage of between 5 and 8 kV with a working 510 distance between 4 and 6 mm. Quantification of the width of cell wall macrofibrils was 511 performed using ImageJ software (Schneider et al., 2012). For the measurements of 512 each macrofibril, a line was drawn parallel to the fibril axis. The length of a second line, 513 perpendicular to the fibril axis line and across the width of the macrofibril, was 514 quantified as the macrofibril width (Figure S2). Each fibril width measurement was 515 standardised for the platinum layer applied during the coating process by subtracting 516 517 the width of the standardised coat from the original measurement. Imaging without the cryo-preservation was performed by visualising hand sectioned platinum coated 518 specimens with the stage maintained at room temperature. For preparation of these 519 samples all freezing steps were omitted. 520

521

522 Sampling and statistical analysis

For spruce, Ginkgo and field grown poplar, stem sections were taken from two 523 individual trees and 150 macrofibrils were measured from three tracheids that had 524 each been coated with platinum separately. Imaging of poplar was performed in 525 technical triplicate from three in vitro grown trees and 150 poplar macrofibrils were 526 measured from three separately coated vessels as for the gymnosperm samples. For 527 Arabidopsis, cryo-SEM imaging of vessels was carried out on three biological 528 replicates, each from separate individuals. 150 macrofibril diameters were measured 529 across the three individuals. 530

Statistical analysis was performed using packages available with R software (Team,
2014). Statistical tests, either Student's T test or ANOVA, used to compare average
measurements for samples are defined in Figure legends. The variance between each
pairwise combination was estimated to be similar with Levene's test.

535 Data statement

All data for the quantification of the macrofibril diameter is presented on Figures forming part of the manuscript. Representative images are provided for each genotype/species for which macrofibril diameter data is provided. All images obtained for the different species and genotypes analysed as part of this manuscript are available from Jan J Lyczakowski (jjl55@cam.ac.uk).

541

542 Accession numbers

543 Mutants in the following genes in the Col-0 ecotype were analysed as part of this 544 study:

- 545 AT5G17420 (*irx*3-7)
- 546 AT2G37090 (*irx9-1*)
- 547 AT1G27440 (irx10-1)
- 548 AT3G55990 (esk1-5)
- 549 AT1G51680 (*4cl1-1*)
- 550 AT2G38080 (lac4-2)
- 551 AT5G22740 (csla2-1)
- 552 AT1G23480 (cs/a3-2) AT5G03760
- 553 (*csla9-1*)
- 554
- 555 List of abbreviations
- 556 1D one dimensional
- 557 AFM atomic force microscopy CesA Cellulose
- 558 synthase cryo-SEM low temperature scanning electron
- 559 microscopy FE-SEM field emission scanning electron
- 560 microscopy
- 561 FT-IR Fourier-transform infrared spectroscopy
- 562 GGM galactoglucomannan
- 563 He-ion Helium ion
- 564 IRX irregular xylem

- 565 [Me]GlcA methylated and unmethylated form of glucuronic acid
- 566 NMR nuclear magnetic resonance
- 567 SANS small angle neutron scattering
- 568 TEM transmission electron microscopy
- 569 WAXS wide angle x-ray scattering
- 570

571 Acknowledgements

We would like to thank Dr Nadine Anders and Dr Henry Temple for helpful discussions 572 and critical reading of the manuscript. This work was supported by the Leverhulme 573 Trust Centre for Natural Material Innovation. Analysis of Arabidopsis mutant plants 574 was supported as part of The Center for LignoCellulose Structure and Formation, an 575 Energy Frontier Research Center funded by the U.S. Department of Energy (DOE), 576 Office of Science, Basic Energy Sciences (BES), under Award # DE-SC0001090. JJL 577 was in receipt of a studentship from the Biotechnology and Biological Sciences 578 Research Council (BBSRC) of the UK as part of the Cambridge BBSRC-DTP 579 Programme (Reference BB/J014540/1). MB is employed in YH's team through the 580 European Research Council Advanced Investigator Grant SYMDEV (No. 323052). YH 581 laboratory is funded by the Finnish Centre of Excellence in Molecular Biology of 582 Primary Producers (Academy of Finland CoE program 2014-2019) (decision 583 #271832); the Gatsby Foundation (GAT3395/PR3); the National Science Foundation 584 585 Biotechnology and Biological Sciences Research Council grant (BB/N013158/1); University of Helsinki (award 799992091), and the European Research Council 586 Advanced Investigator Grant SYMDEV (No. 323052). OMT was a recipient of an 587 iCASE studentship from the BBSRC (Reference BB/M015432/1). We thank Gareth 588

Evans for help with cryo-SEM sample preparation. The cryo-SEM facility at the Sainsbury Laboratory is supported by the Gatsby Charitable Foundation. We are grateful to Cambridge University Botanic Garden for access to the *Populus tremula* and *Ginkgo biloba* collections.

593 The authors declare no conflict of interest.

594

595 Author contributions

596 JJL designed the study, conducted the experiments, analysed the data and wrote the 597 paper. MB performed poplar imaging experiments, analysed the data and wrote the 598 paper. OMT analysed the data and wrote the paper. YH contributed to data analysis 599 and manuscript preparation, RW designed the study, conducted experiments, 600 analysed the data and wrote the paper. PD designed the study and contributed to data 601 analysis and manuscript preparation.

- 602
- 603
- 604

605 Short legends for supporting information:

- ⁶⁰⁶ Figure S1: Overview of the cryo-SEM procedure.
- Figure S2: Measurement of macrofibril diameter.
- ⁶⁰⁸ Figure S3: Cryo-SEM analysis of Ginkgo cell walls.
- Figure S4: Comparison of macrofibril diameter in Arabidopsis, poplar, spruce andGinkgo.
- Figure S5: Imaging of macrofibrils in field grown poplar.
- Figure S6: Analysis of native Arabidopsis samples without the cryo-preservation
- 613 protocol.
- Figure S7: Cryo-SEM analysis of vessel collapse and primary cell wall cellulose in
- 615 *irx3* Arabidopsis plants.
- 616

617 **References**

- ABE, H., FUNADA, R., OHTANI, J. & FUKAZAWA, K. 1997. Changes in the
 arrangement of cellulose microfibrils associated with the cessation of cell
 expansion in tracheids. *Trees-Structure and Function*, 11, 328-332.
- BAUER, S., VASU, P., PERSSON, S., MORT, A. J. & SOMERVILLE, C. R. 2006.
 Development and application of a suite of polysaccharide-degrading enzymes

623	for analyzing plant cell walls. Proceedings of the National Academy of
624	Sciences of the United States of America, 103, 11417-11422.
625	BERTHET, S., DEMONT-CAULET, N., POLLET, B., BIDZINSKI, P., CEZARD, L., LE
626	BRIS, P., BORREGA, N., HERVE, J., BLONDET, E., BALZERGUE, S.,
627	LAPIERRE, C. & JOUANIN, L. 2011. Disruption of LACCASE4 and 17
628	Results in Tissue-Specific Alterations to Lignification of Arabidopsis thaliana
629	Stems. Plant Cell, 23, 1124-1137.
630	BONAWITZ, N. D. & CHAPPLE, C. 2010. The Genetics of Lignin Biosynthesis:
631	Connecting Genotype to Phenotype. Annual Review of Genetics, Vol 44, 44,
632	337-363.
633	BOURIAUD, O., LEBAN, J. M., BERT, D. & DELEUZE, C. 2005. Intra-annual
634	variations in climate influence growth and wood density of Norway spruce.
635	Tree Physiology, 25, 651-660.
636	BROMLEY, J. R., BUSSE-WICHER, M., TRYFONA, T., MORTIMER, J. C., ZHANG,
637	Z., BROWN, D. M. & DUPREE, P. 2013. GUX1 and GUX2
638	glucuronyltransferases decorate distinct domains of glucuronoxylan with
639	different substitution patterns. <i>Plant Journal</i> , 74, 423-434.
640	BROWN, D. M., GOUBET, F., VICKY, W. W. A., GOODACRE, R., STEPHENS, E.,
641	DUPREE, P. & TURNER, S. R. 2007. Comparison of five xylan synthesis
642	mutants reveals new insight into the mechanisms of xylan synthesis. <i>Plant</i>
643	Journal, 52, 1154-1168.
644	BROWN, D. M., ZEEF, L. A. H., ELLIS, J., GOODACRE, R. & TURNER, S. R. 2005.
645	Identification of novel genes in Arabidopsis involved in secondary cell wall
646	formation using expression profiling and reverse genetics. <i>Plant Cell</i> , 17, 2281-2295.
647	BUSSE-WICHER, M., GOMES, T. C. F., TRYFONA, T., NIKOLOVSKI, N., STOTT,
648	
649	K., GRANTHAM, N. J., BOLAM, D. N., SKAF, M. S. & DUPREE, P. 2014. The
650	pattern of xylan acetylation suggests xylan may interact with cellulose
651 (52	microfibrils as a twofold helical screw in the secondary plant cell wall of
652	Arabidopsis thaliana. <i>Plant Journal</i> , 79, 492-506.
653	BUSSE-WICHER, M., GRANTHAM, N. J., LYCZAKOWSKI, J. J., NIKOLOVSKI, N. &
654	DUPREE, P. 2016a. Xylan decoration patterns and the plant secondary cell wall
655	molecular architecture. <i>Biochemical Society Transactions</i> , 44, 74-78. BUSSE-
656	WICHER, M., LI, A., SILVEIRA, R. L., PEREIRA, C. S., TRYFONA, T., GOMES, T.
657	C. F., SKAF, M. S. & DUPREE, P. 2016b. Evolution of Xylan Substitution Patterns in
658	Gymnosperms and Angiosperms: Implications for Xylan Interaction with Cellulose.
659	Plant Physiology, 171, 2418-2431.
660	CASDORFF, K., KEPLINGER, T., BURGERT, I. 2017. Nono-mechanical
661	characterisation of the wood cell wall by AFM studies: comparison between
662	AC- and QI [™] mode. <i>Plant Methods,</i> 13, 60.
663	COCHARD, H., FROUX, F., MAYR, F. F. S. & COUTAND, C. 2004. Xylem wall
664	collapse in water-stressed pine needles. <i>Plant Physiology</i> , 134, 401-408.
665	COSGROVE, D. J. 2014. Re-constructing our models of cellulose and primary cell
666	wall assembly. Current Opinion in Plant Biology, 22, 121-131.
667	DICK-PEREZ, M., ZHANG, Y. A., HAYES, J., SALAZAR, A., ZABOTINA, O. A.,
668	HONG, M. 2011. Structure and interactions of plant cell-wall polysaccharides
669	by two- and three-dimensional magic-angle-spinning solid-state NMR.
670	<i>Biochemistry,</i> 50, 989-1000.

DONALDSON, L. 2007. Cellulose microfibril aggregates and their size variation with 671 cell wall type. Wood Science and Technology, 41, 443-460. 672 ELBAUM, R., GORB, S., FRATZL, P. 2008. Structures in the cell wall that enable 673 hygroscopic movement of wheat awns. Journal of Structural Biology, 164, 674 101-107. 675 FAHLEN, J. & SALMEN, L. 2002. On the Lamellar Structure of the Tracheid Cell 676 Wall. Plant Biology, 4, 339-345. 677 FAVERY, B., RYAN, E., FOREMAN, J., LINSTEAD, P., BOUDONCK, K., STEER, 678 M., SHAW, P. & DOLAN, L. 2001. KOJAK encodes a cellulose synthase-like 679 protein required for root hair cell morphogenesis in Arabidopsis. Genes & 680 Development, 15, 79-89. 681 FERNANDES, A. N., THOMAS, L. H., ALTANER, C. M., CALLOW, P., FORSYTH, 682 V. T., APPERLEY, D. C., KENNEDY, C. J. & JARVIS, M. C. 2011. 683 Nanostructure of cellulose microfibrils in spruce wood. Proceedings of the 684 National Academy of Sciences of the United States of America, 108, 685 E1195E1203. 686 FROMM, J., ROCKEL, B., LAUTNER, S., WINDEISEN, E. & WANNER, G. 2003. 687 Lignin distribution in wood cell walls determined by TEM and backscattered 688 SEM techniques. Journal of Structural Biology, 143, 77-84. 689 690 FUJITA, M., HIMMELSPACH, R., WARD, J., WHITTINGTON, A., HASENBEIN, N., LIU, C., TRUONG, T. T., GALWAY, M. E., MANSFIELD, S. D., HOCART, C. 691 H. & WASTENEYS, G. O. 2013. The anisotropy1 D604N Mutation in the 692 Arabidopsis Cellulose Synthase1 Catalytic Domain Reduces Cell Wall 693 Crystallinity and the Velocity of Cellulose Synthase Complexes. Plant 694 Physiology, 162, 74-85. 695 696 GIERLINGER, N. 2018. New insights into plant cell walls by vibrational microspectroscopy. Applied Spectroscopy Reviews, 53, 517-551. 697 GONNEAU, M., DESPREZ, T., GUILLOT, A., VERNHETTES, S. & HOFTE, H. 2014. 698 Catalytic Subunit Stoichiometry within the Cellulose Synthase Complex. Plant 699 Physiology, 166, 1709-1712. 700 GOUBET, F., BARTON, C. J., MORTIMER, J. C., YU, X. L., ZHANG, Z. N., MILES, 701 702 G. P., RICHENS, J., LIEPMAN, A. H., SEFFEN, K. & DUPREE, P. 2009. Cell wall glucomannan in Arabidopsis is synthesised by CSLA 703 704 glycosyltransferases, and influences the progression of embryogenesis. *Plant* Journal, 60, 527-538. 705 706 GRANTHAM, N. J., WURMAN-RODRICH, J., TERRETT, O. M., LYCZAKOWSKI, J. 707 J., STOTT, K., IUGA, D., SIMMONS, T. J., DURAND-TARDIF, M., BROWN, S. P., DUPREE, R., BUSSE-WICHER, M. & DUPREE, P. 2017. An even 708 pattern of xylan substitution is critical for interaction with cellulose in plant cell 709 walls. Nature Plants, 3, 859-865. 710 HILL, J. L., HAMMUDI, M. B. & TIEN, M. 2014. The Arabidopsis Cellulose Synthase 711 Complex: A Proposed Hexamer of CESA Trimers in an Equimolar 712 713 Stoichiometry. *Plant Cell*, 26, 4834-4842. HIMMELSPACH, R., WILLIAMSON, R. E. & WASTENEYS, G. O. 2003. Cellulose 714 microfibril alignment recovers from DCB-induced disruption despite 715 microtubule disorganization. Plant Journal, 36, 565-575. 716

717 718	JARVIS, M. C. 2018. Structure of native cellulose microfibrils, the starting point for nanocellulose manufacture. <i>Philosophical transactions. Series A</i> ,
719	Mathematical, physical, and engineering sciences, 376.
720	JOENS, M. S., HUYNH, C., KASUBOSKI, J. M., FERRANTI, D., SIGAL, Y. J.,
721	ZEITVOGEL, F., OBST, M., BURKHARDT, C. J., CURRAN, K. P.,
722	CHALASANI, S. H., STERN, L. A., GOETZE, B. & FITZPATRICK, J. A. J.
723	2013. Helium Ion Microscopy (HIM) for the imaging of biological samples at
724	sub-nanometer resolution. Scientific Reports, 3.KANG, X., KIRUI, A.,
725	DICKWELLA WIDANAGE, M. C., MENTINK-VIGIER, F., COSGROVE, D. J.,
726	WANG, T. 2019. Lignin-polysaccharide interactions in plant secondary cell
727	walls revealed by solid-state NMR. Nature Communications, 10, 347.
728	KUMAR, M. & TURNER, S. 2015. Protocol: a medium-throughput method for
729	determination of cellulose content from single stem pieces of Arabidopsis
730	thaliana. <i>Plant Methods,</i> 11.
731	LEFEBVRE, V., FORTABAT, M. N., DUCAMP, A., NORTH, H. M.,
732	MAIAGRONDARD, A., TROUVERIE, J., BOURSIAC, Y., MOUILLE, G. &
733	DURAND-TARDIF, M. 2011. ESKIMO1 Disruption in Arabidopsis Alters
734	Vascular Tissue and Impairs Water Transport. Plos One, 6.
735	LI, S. D., BASHLINE, L., ZHENG, Y. Z., XIN, X. R., HUANG, S. X., KONG, Z. S.,
736	KIM, S. H., COSGROVE, D. J. & GU, Y. 2016. Cellulose synthase complexes
737	act in a concerted fashion to synthesize highly aggregated cellulose in
738	secondary cell walls of plants. Proceedings of the National Academy of
739	Sciences of the United States of America, 113, 11348-11353.
740	LI, Y., KIM, J. I., PYSH, L. & CHAPPLE, C. 2015. Four Isoforms of Arabidopsis
741	4Coumarate: CoA Ligase Have Overlapping yet Distinct Roles in
742	Phenylpropanoid Metabolism. Plant Physiology, 169, 2409-2421.
743	LOQUE, D., SCHELLER, H. V. & PAULY, M. 2015. Engineering of plant cell walls for
744	enhanced biofuel production. <i>Current Opinion in Plant Biology</i> , 25, 151-161.
745	LYCZAKOWSKI, J. J., WICHER, K. B., TERRETT, O. M., FARIA-BLANC, N., YU, X.
746	L., BROWN, D., KROGH, K., DUPREE, P. & BUSSE-WICHER, M. 2017.
747	Removal of glucuronic acid from xylan is a strategy to improve the conversion
748	of plant biomass to sugars for bioenergy. <i>Biotechnology for Biofuels</i> , 10.
749	MAKINEN, H., SARANPAA, P. & LINDER, S. 2002. Wood-density variation of
750	Norway spruce in relation to nutrient optimization and fibre dimensions.
751	Canadian Journal of Forest Research-Revue Canadienne De Recherche
752	Forestiere, 32, 185-194.
753	MARGA, F., GRANDBOIS, M., COSGROVE, D. J. & BASKIN, T. I. 2005. Cell wall
754 755	extension results in the coordinate separation of parallel microfibrils: evidence from scanning electron microscopy and atomic force microscopy. <i>Plant</i>
756	Journal, 43, 181-190.
757	MARTINEZ-ABAD, A., BERGLUND, J., TORIZ, G., GATENHOLM, P.,
758	HENRIKSSON, G., LINDSTROM, M., WOHLERT, J. & VILAPLANA, F. 2017.
759	Regular Motifs in Xylan Modulate Molecular Flexibility and Interactions with
760	Cellulose Surfaces. <i>Plant Physiology</i> , 175, 1579-1592.
761	NIKLAS, K. 2004. The cell walls that bind the tree of life. <i>BioScience</i> , 54, 831-841.
762	NISHIMURA, H., KAMIYA, A., NAGATA, T., KATAHIRA, M. & WATANABE, T. 2018.
763	Direct evidence for alpha ether linkage between lignin and carbohydrates in
764	wood cell walls. <i>Scientific Reports</i> , 8.
764	wood cell walls. Scientific Reports, 8.

PAN, Y. D., BIRDSEY, R. A., FANG, J. Y., HOUGHTON, R., KAUPPI, P. E., KURZ, 765 W. A., PHILLIPS, O. L., SHVIDENKO, A., LEWIS, S. L., CANADELL, J. G., 766 CIAIS, P., JACKSON, R. B., PACALA, S. W., MCGUIRE, A. D., PIAO, S. L., 767 RAUTIAINEN, A., SITCH, S. & HAYES, D. 2011. A Large and Persistent 768 Carbon Sink in the World's Forests. Science, 333, 988-993. 769 PAULY, M. & KEEGSTRA, K. 2008, Cell-wall carbohydrates and their modification 770 as a resource for biofuels. Plant Journal, 54, 559-568. 771 772 PURBASHA, S., BOSNEAGA, E. AUER, M. 2009. Plant cell walls throughout 773 evolution: towards a molecular understanding of their design principles. Journal of Experimental Botany, 60, 3615-3635. 774 RALPH, J., LUNDQUIST, K., BRUNOW, G., LU, F., KIM, H., SCHATZ, P. F., 775 MARITA, J. M., HATFIELD, R. D., RALPH, S. A., CHRISTENSEN, J. H., 776 BOERJAN, W. 2004. Lignins: natural polymers from oxidative coupling of 777 4hvdroxyphenyl- propanoids. Phytochemistry Reviews, 3, 29-60. 778 RAMAGE, M. H., BURRIDGE, H., BUSSE-WICHER, M., FEREDAY, G., 779 REYNOLDS, T., SHAH, D. U., WU, G. L., YU, L., FLEMING, P., 780 DENSLEYTINGLEY, D., ALLWOOD, J., DUPREE, P., LINDEN, P. F. & 781 SCHERMAN, O. 2017. The wood from the trees: The use of timber in 782 construction. Renewable & Sustainable Energy Reviews, 68, 333-359. 783 REFREGIER, G., PELLETIER, S., JAILLARD, D. & HOFTE, H. 2004. Interaction 784 between wall deposition and cell elongation in dark-grown hypocotyl cells in 785 Arabidopsis. Plant Physiology, 135, 959-968. 786 SANSINENA, M., SANTOS, M. V., ZARITZKY, N., CHIRIFE, J. 2012. Comparison of 787 heat transfer in liquid and slush nitrogen by numerical simulation of cooling 788 rates for French straws used for sperm cryopreservation. Theriogenology, 77, 789 790 1717-1721. 791 SCHELLER, H. V. & ULVSKOV, P. 2010. Hemicelluloses. Annual Review of Plant Biology, Vol 61, 61, 263-289. 792 SCHNEIDER, C. A., RASBAND, W. S. & ELICEIRI, K. W. 2012. NIH Image to 793 ImageJ: 25 years of image analysis. Nature Methods, 9, 671-675. 794 SCHWEINGRUBER, F. H. 2007. Wood structure and environment, Berlin, Springer. 795 796 SCZOSTAK, A. 2009. Cotton Linters: An Alternative Cellulosic Raw Material. 797 Macromolecular Symposia, 280, 45-53. SIMMONS, T. J., MORTIMER, J. C., BERNARDINELLI, O. D., POPPLER, A. C., 798 BROWN, S. P., DEAZEVEDO, E. R., DUPREE, R. & DUPREE, P. 2016. 799 Folding of xylan onto cellulose fibrils in plant cell walls revealed by solid-state 800 NMR. Nature Communications, 7. 801 TAKENAKA, Y., WATANABE, Y., SCHUETZ, M., UNDA, F., HILL, J., PHOOKAEW, 802 P., YONEDA, A., MANSFIELD, S. D., SAMUELS, L., OHTANI, M & DEMURA, 803 T. 2018. Patterned deposition of xylan and lignin is independent from that of 804 the secondary wall cellulose of Arabidopsis xylem vessels. Plant Cell, 30, 805 2663-2676. 806 TAYLOR, N. G., SCHEIBLE, W. R., CUTLER, S., SOMERVILLE, C. R. & TURNER, 807 S. R. 1999. The irregular xylem3 locus of arabidopsis encodes a cellulose 808 809 synthase required for secondary cell wall synthesis. Plant Cell, 11, 769-779. TEAM, R. C. 2014. R: A language and environment for statistical computing. 810 [Online]. Vienna Austria. Available: http://www.R-project.org/ [Accessed]. 811

 WESTERMARK, U. 2009. Nanostructural assembly of cellulose, hemicellulose, and lignin in the middle layer of secondary wall of ginkgo tracheid. <i>Journal of Wood Science</i>, 55, 409-416. TERRETT, O. M., DUPREE, P. 2019. Covalent interactions between lignin and hemicelluloses in plant secondary cell walls. <i>Current Opinion in Biotechnology</i>, 56, 97-104. THOMAS, L. H., ALTANER, C. M. & JARVIS, M. C. 2013. Identifying multiple forms of lateral disorder in cellulose fibres. <i>Journal of Applied Crystallography</i>, 46, 972-979. THOMAS, L. H., FORSYTH, V. T., MARTEL, A., GRILLO, I., ALTANER, C. M. & JARVIS, M. C. 2014. Structure and spacing of cellulose microfibrils in woody cell walls of dicots. <i>Cellulose</i>, 21, 3887-3895. THOMAS, L. H., FORSYTH, V. T., MARTEL, A., GRILLO, I., ALTANER, C. M. & JARVIS, M. C. 2015. Diffraction evidence for the structure of cellulose microfibrils in bamboo, a model for grass and cereal celluloses. <i>Bmc Plant Biology</i>, 15. TURNER, S. & KUMAR, M. 2017. Cellulose synthase complex organization and cellulose microfibril structure. <i>Philosophical Transactions of the Royal Society</i> <i>A</i>, 376. TURNER, S. R. & SOMERVILLE, C. R. 1997. Collapsed xylem phenotype of Arabidopsis identifies mutants deficient in cellulose deposition in the secondary cell wall. <i>Plant Cell</i>, 9, 689-701. VANHOLME, R., STORME, V., VANHOLME, B., SUNDINI, L., CHRISTENSEN, J. H., GOEMINNE, G., HALPIN, C., ROHDE, A., MORREEL, K. & BOERJAN, W. 2012. A Systems Biology View of Responses to Lignin Biosynthesis Perturbations in Arabidopsis. <i>Plant Cell</i>, 24, 3506-3529. WHITNEY, S. E. C., BRIGHAM, J. E., DARKE, A. H., REID, J. S. G. & GIDLEY, M. J. 1998. Structural aspects of the interaction of mannan-based polysaccharides with bacterial cellulose. <i>Carbohydrate Research</i>, 307, 29309. XIONG, G., CHENG, K. & PAULY, M. Xylan O-Acetylation Impacts Xylem Development and Enzymatic Recalcitrance as Indicated by the A	812	TERASHIMA, N., KITANO, K., KOJIMA, M., YOSHIDA, M., YAMAMOTO, H. &
 tracheid. <i>Journal of Wood Science</i>, 55, 409-416. TERRETT, O. M., DUPREE, P. 2019. Covalent interactions between lignin and hemicelluloses in plant secondary cell walls. <i>Current Opinion in Biotechnology</i>, 56, 97-104. THOMAS, L. H., ALTANER, C. M. & JARVIS, M. C. 2013. Identifying multiple forms of lateral disorder in cellulose fibres. <i>Journal of Applied Crystallography</i>, 46, 972-979. THOMAS, L. H., FORSYTH, V. T., MARTEL, A., GRILLO, I., ALTANER, C. M. & JARVIS, M. C. 2014. Structure and spacing of cellulose microfibrils in woody cell walls of dicots. <i>Cellulose</i>, 21, 3887-3895. THOMAS, L. H., FORSYTH, V. T., MARTEL, A., GRILLO, I., ALTANER, C. M. & JARVIS, M. C. 2015. Diffraction evidence for the structure of cellulose microfibrils in bamboo, a model for grass and cereal celluloses. <i>Bmc Plant Biology</i>, 15. TURNER, S. & KUMAR, M. 2017. Cellulose synthase complex organization and cellulose microfibril structure. <i>Philosophical Transactions of the Royal Society</i> <i>A</i>, 376. TURNER, S. R. & SOMERVILLE, C. R. 1997. Collapsed xylem phenotype of Arabidopsis identifies mutants deficient in cellulose deposition in the secondary cell wall. <i>Plant Cell</i>, 9, 689-701. VANHOLME, R., DEMEDTS, B., MORREEL, K., RALPH, J., BOERJAN, W. 2010. Lignin biosynthesis and structure. <i>Plant Physiology</i>, 132, 1781-1789. VANHOLME, R., STORME, V., VANHOLME, B., SUNDIN, L., CHRISTENSEN, J. H., GOEMINNE, G., HALPIN, C., ROHDE, A., MORREEL, K. & & BOERJAN, W. 2012. A Systems Biology View of Responses to Lignin Biosynthesis Perturbations in Arabidopsis. <i>Plant Cell</i>, 24, 3506-3529. WHITNEY, S. E. C., BRIGHAM, J. E., DARKE, A. H., REID, J. S. G. & GIDLEY, M. J. 1998. Structural aspects of the interaction of mannan-based polysaccharides with bacterial cellulose. <i>Carbohydrate Research</i>, 307, 299309. XIONG, G., CHENG, K. & PAULY, M. Xylan O-Acetylation Impacts Xylem Development and Enzymatic Recalcitrance	813	WESTERMARK, U. 2009. Nanostructural assembly of cellulose,
 TERRETT, O. M., DUPREE, P. 2019. Covalent interactions between lignin and hemicelluloses in plant secondary cell walls. <i>Current Opinion in</i> <i>Biotechnology</i>, 56, 97-104. THOMAS, L. H., ALTANER, C. M. & JARVIS, M. C. 2013. Identifying multiple forms of lateral disorder in cellulose fibres. <i>Journal of Applied Crystallography</i>, 46, 972-979. THOMAS, L. H., FORSYTH, V. T., MARTEL, A., GRILLO, I., ALTANER, C. M. & JARVIS, M. C. 2014. Structure and spacing of cellulose microfibrils in woody cell walls of dicots. <i>Cellulose</i>, 21, 3887-3895. THOMAS, L. H., FORSYTH, V. T., MARTEL, A., GRILLO, I., ALTANER, C. M. & JARVIS, M. C. 2015. Diffraction evidence for the structure of cellulose microfibrils in bamboo, a model for grass and cereal celluloses. <i>Bmc Plant Biology</i>, 15. TURNER, S. & KUMAR, M. 2017. Cellulose synthase complex organization and cellulose microfibril structure. <i>Philosophical Transactions of the Royal Society</i> <i>A</i>, 376. TURNER, S. R. & SOMERVILLE, C. R. 1997. Collapsed xylem phenotype of Arabidopsis identifies mutants deficient in cellulose deposition in the secondary cell wall. <i>Plant Cell</i>, 9, 689-701. VANHOLME, R., DEMEDTS, B., MORREEL, K., RALPH, J., BOERJAN, W. 2010. Lignin biosynthesis and structure. <i>Plant Physiology</i>, 132, 1781-1789. VANHOLME, R., STORME, V., VANHOLME, B., SUNDIN, L., CHRISTENSEN, J. H., GOEMINNE, G., HALPIN, C., ROHDE, A., MORREL, K. & BOERJAN, W. 2012. A Systems Biology View of Responses to Lignin Biosynthesis Perturbations in Arabidopsis. <i>Plant Cell</i>, 24, 3506-3529. WHITNEY, S. E. C., BRIGHAM, J. E., DARKE, A. H., REID, J. S. G. & GIDLEY, M. J. 1998. Structural aspects of the interaction of mannan-based polysaccharides with bacterial cellulose. <i>Carbohydrate Research</i>, 307, 299309. XIONG, G., CHENG, K. & PAULY, M. Xylan O-Acetylation Impacts Xylem Development and Enzymatic Recalcitrance as Indicated by the Arabidopsis Mutant tbl29. <i>Molecular Plant</i>	814	hemicellulose, and lignin in the middle layer of secondary wall of ginkgo
 hemicelluloses in plant secondary cell walls. <i>Current Opinion in</i> <i>Biotechnology</i>, 56, 97-104. THOMAS, L. H., ALTANER, C. M. & JARVIS, M. C. 2013. Identifying multiple forms of lateral disorder in cellulose fibres. <i>Journal of Applied Crystallography</i>, 46, 972-979. THOMAS, L. H., FORSYTH, V. T., MARTEL, A., GRILLO, I., ALTANER, C. M. & JARVIS, M. C. 2014. Structure and spacing of cellulose microfibrils in woody cell walls of dicots. <i>Cellulose</i>, 21, 3887-3895. THOMAS, L. H., FORSYTH, V. T., MARTEL, A., GRILLO, I., ALTANER, C. M. & JARVIS, M. C. 2015. Diffraction evidence for the structure of cellulose microfibrils in bamboo, a model for grass and cereal celluloses. <i>Bmc Plant Biology</i>, 15. TURNER, S. & KUMAR, M. 2017. Cellulose synthase complex organization and cellulose microfibril structure. <i>Philosophical Transactions of the Royal Society</i> <i>A</i>, 376. TURNER, S. R. & SOMERVILLE, C. R. 1997. Collapsed xylem phenotype of Arabidopsis identifies mutants deficient in cellulose deposition in the secondary cell wall. <i>Plant Cell</i>, 9, 689-701. VANHOLME, R., DEMEDTS, B., MORREEL, K., RALPH, J., BOERJAN, W. 2010. Lignin biosynthesis and structure. <i>Plant Physiology</i>, 132, 1781-1789. VANHOLME, R., STORME, V., VANHOLME, B., SUNDIN, L., CHRISTENSEN, J. H., GOEMINNE, G., HALPIN, C., ROHDE, A., MORREEL, K. & BOERJAN, W. 2012. A Systems Biology View of Responses to Lignin Biosynthesis Perturbations in Arabidopsis. <i>Plant Cell</i>, 24, 3506-3529. WHITNEY, S. E. C., BRIGHAM, J. E., DARKE, A. H., REID, J. S. G. & GIDLEY, M. J. 1998. Structural aspects of the interaction of mannan-based polysaccharides with bacterial cellulose. <i>Carbohydrate Research</i>, 307, 299309. XIONG, C., CHENG, K. & PAULY, M. Xylan O-Acetylation Impacts Xylem Development and Enzymatic Recalcitrance as Indicated by the Arabidopsis Mutant tbl29. <i>Molecular Plant</i>, 6, 1373-1375. YU, L., LYCZAKOWSKI, J. J., PEREIRA, C. S.,	815	tracheid. Journal of Wood Science, 55, 409-416.
 Biotechnology, 56, 97-104. THOMAS, L. H., ALTANER, C. M. & JARVIS, M. C. 2013. Identifying multiple forms of lateral disorder in cellulose fibres. <i>Journal of Applied Crystallography</i>, 46, 972-979. THOMAS, L. H., FORSYTH, V. T., MARTEL, A., GRILLO, I., ALTANER, C. M. & JARVIS, M. C. 2014. Structure and spacing of cellulose microfibrils in woody cell walls of dicots. <i>Cellulose</i>, 21, 3887-3895. THOMAS, L. H., FORSYTH, V. T., MARTEL, A., GRILLO, I., ALTANER, C. M. & JARVIS, M. C. 2015. Diffraction evidence for the structure of cellulose microfibrils in bamboo, a model for grass and cereal celluloses. <i>Bmc Plant Biology</i>, 15. TURNER, S. & KUMAR, M. 2017. Cellulose synthase complex organization and cellulose microfibril structure. <i>Philosophical Transactions of the Royal Society A</i>, 376. TURNER, S. R. & SOMERVILLE, C. R. 1997. Collapsed xylem phenotype of Arabidopsis identifies mutants deficient in cellulose deposition in the secondary cell wall. <i>Plant Cell</i>, 9, 689-701. VANHOLME, R., DEMEDTS, B., MORREEL, K., RALPH, J., BOERJAN, W. 2010. Lignin biosynthesis and structure. <i>Plant Physiology</i>, 132, 1781-1789. VANHOLME, R., STORME, V., VANHOLME, B., SUNDIN, L., CHRISTENSEN, J. H., GOEMINNE, G., HALPIN, C., ROHDE, A., MORREEL, K. & BOERJAN, W. 2012. A Systems Biology View of Responses to Lignin Biosynthesis Perturbations in Arabidopsis. <i>Plant Cell</i>, 24, 3506-3529. WHITNEY, S. E. C., BRIGHAM, J. E., DARKE, A. H., REID, J. S. G. & GIDLEY, M. J. 1998. Structural aspects of the interaction of mannan-based polysaccharides with bacterial cellulose. <i>Carbohydrate Research</i>, 307, 29309. XIONG, G., CHENG, K. & PAULY, M. Xylan O-Acetylation Impacts Xylem Development and Enzymatic Recalcitrance as Indicated by the Arabidopsis Mutant tbl29. <i>Molecular Plant</i>, 6, 1373-1375. YU, L., LYCZAKOWSKI, J. J., PEREIRA, C. S., KOTAKE, T., YU, X., LI, A., MOGELSVANG, S., SKAF, M. S. & DUPREE, P. 201	816	TERRETT, O. M., DUPREE, P. 2019. Covalent interactions between lignin and
 Biotechnology, 56, 97-104. THOMAS, L. H., ALTANER, C. M. & JARVIS, M. C. 2013. Identifying multiple forms of lateral disorder in cellulose fibres. <i>Journal of Applied Crystallography</i>, 46, 972-979. THOMAS, L. H., FORSYTH, V. T., MARTEL, A., GRILLO, I., ALTANER, C. M. & JARVIS, M. C. 2014. Structure and spacing of cellulose microfibrils in woody cell walls of dicots. <i>Cellulose</i>, 21, 3887-3895. THOMAS, L. H., FORSYTH, V. T., MARTEL, A., GRILLO, I., ALTANER, C. M. & JARVIS, M. C. 2015. Diffraction evidence for the structure of cellulose microfibrils in bamboo, a model for grass and cereal celluloses. <i>Bmc Plant Biology</i>, 15. TURNER, S. & KUMAR, M. 2017. Cellulose synthase complex organization and cellulose microfibril structure. <i>Philosophical Transactions of the Royal Society A</i>, 376. TURNER, S. R. & SOMERVILLE, C. R. 1997. Collapsed xylem phenotype of Arabidopsis identifies mutants deficient in cellulose deposition in the secondary cell wall. <i>Plant Cell</i>, 9, 689-701. VANHOLME, R., DEMEDTS, B., MORREEL, K., RALPH, J., BOERJAN, W. 2010. Lignin biosynthesis and structure. <i>Plant Physiology</i>, 132, 1781-1789. VANHOLME, R., STORME, V., VANHOLME, B., SUNDIN, L., CHRISTENSEN, J. H., GOEMINNE, G., HALPIN, C., ROHDE, A., MORREEL, K. & BOERJAN, W. 2012. A Systems Biology View of Responses to Lignin Biosynthesis Perturbations in Arabidopsis. <i>Plant Cell</i>, 24, 3506-3529. WHITNEY, S. E. C., BRIGHAM, J. E., DARKE, A. H., REID, J. S. G. & GIDLEY, M. J. 1998. Structural aspects of the interaction of mannan-based polysaccharides with bacterial cellulose. <i>Carbohydrate Research</i>, 307, 29309. XIONG, G., CHENG, K. & PAULY, M. Xylan O-Acetylation Impacts Xylem Development and Enzymatic Recalcitrance as Indicated by the Arabidopsis Mutant tbl29. <i>Molecular Plant</i>, 6, 1373-1375. YU, L., LYCZAKOWSKI, J. J., PEREIRA, C. S., KOTAKE, T., YU, X., LI, A., MOGELSVANG, S., SKAF, M. S. & DUPREE, P. 201	817	hemicelluloses in plant secondary cell walls. Current Opinion in
 THOMAS, L. H., ALTANÉR, C. M. & JARVIS, M. C. 2013. Identifying multiple forms of lateral disorder in cellulose fibres. <i>Journal of Applied Crystallography</i>, 46, 972-979. THOMAS, L. H., FORSYTH, V. T., MARTEL, A., GRILLO, I., ALTANER, C. M. & JARVIS, M. C. 2014. Structure and spacing of cellulose microfibrils in woody cell walls of dicots. <i>Cellulose</i>, 21, 3887-3895. THOMAS, L. H., FORSYTH, V. T., MARTEL, A., GRILLO, I., ALTANER, C. M. & JARVIS, M. C. 2015. Diffraction evidence for the structure of cellulose microfibrils in bamboo, a model for grass and cereal celluloses. <i>Bmc Plant Biology</i>, 15. TURNER, S. & KUMAR, M. 2017. Cellulose synthase complex organization and cellulose microfibril structure. <i>Philosophical Transactions of the Royal Society</i> <i>A</i>, 376. TURNER, S. R. & SOMERVILLE, C. R. 1997. Collapsed xylem phenotype of Arabidopsis identifies mutants deficient in cellulose deposition in the secondary cell wall. <i>Plant Cell</i>, 9, 689-701. VANHOLME, R., STORME, V., VANHOLME, B., SUNDIN, L., CHRISTENSEN, J. H., GOEMINNE, G., HALPIN, C., ROHDE, A., MORREEL, K. & BOERJAN, W. 2010. Lignin biosynthesis and structure. <i>Plant Physiology</i>, 132, 1781-1789. VANHOLME, R., STORME, V., VANHOLME, A. H., REID, J. S. G. & GIDLEY, M. J. 1998. Structural aspects of the interaction of mannan-based polysaccharides with bacterial cellulose. <i>Carbohydrate Research</i>, 307, 299309. XIONG, G., CHENG, K. & PAULY, M. Xylan O-Acetylation Impacts Xylem Development and Enzymatic Recalcitrance as Indicated by the Arabidopsis Mutant tbl29. <i>Molecular Plant</i>, 6, 1373-1375. YU, L., LYCZAKOWSKI, J. J., PEREIRA, C. S., KOTAKE, T., YU, X., LI, A., MOGELSVANG, S., SKAF, M. S. & DUPREE, P. 2018. The patterned structure of galactoglucomannan suggests it may bind to cellulose in seed mucilage. <i>Plant Physiology</i>, 178, 1011-1026. ZHANG, X. Y., DOMINGUEZ, P. G., KUMAR, M., BYGDELL, J., MIROSHNINCHENKO, S., SUNDBERG, B., WI		
 of lateral disorder in cellulose fibres. <i>Journal of Applied Crystallography</i>, 46, 972-979. THOMAS, L. H., FORSYTH, V. T., MARTEL, A., GRILLO, I., ALTANER, C. M. & JARVIS, M. C. 2014. Structure and spacing of cellulose microfibrils in woody cell walls of dicots. <i>Cellulose</i>, 21, 3887-3895. THOMAS, L. H., FORSYTH, V. T., MARTEL, A., GRILLO, I., ALTANER, C. M. & JARVIS, M. C. 2015. Diffraction evidence for the structure of cellulose microfibrils in bamboo, a model for grass and cereal celluloses. <i>Bmc Plant Biology</i>, 15. TURNER, S. & KUMAR, M. 2017. Cellulose synthase complex organization and cellulose microfibrils in tructure. <i>Philosophical Transactions of the Royal Society A</i>, 376. TURNER, S. R. & SOMERVILLE, C. R. 1997. Collapsed xylem phenotype of Arabidopsis identifies mutants deficient in cellulose deposition in the secondary cell wall. <i>Plant Cell</i>, 9, 689-701. VANHOLME, R., DEMEDTS, B., MORREEL, K., RALPH, J., BOERJAN, W. 2010. Lignin biosynthesis and structure. <i>Plant Physiology</i>, 132, 1781-1789. VANHOLME, R., STORME, V., VANHOLME, B., SUNDIN, L., CHRISTENSEN, J. H., GOEMINNE, G., HALPIN, C., ROHDE, A., MORREEL, K. & BOERJAN, W. 2012. A Systems Biology View of Responses to Lignin Biosynthesis Perturbations in Arabidopsis. <i>Plant Cell</i>, 24, 3506-3529. WHITNEY, S. E. C., BRIGHAM, J. E., DARKE, A. H., REID, J. S. G. & GIDLEY, M. J. 1998. Structural aspects of the interaction of mannan-based polysaccharides with bacterial cellulose. <i>Carbohydrate Research</i>, 307, 299309. XIONG, G., CHENG, K. & PAULY, M. Xylan O-Acetylation Impacts Xylem Development and Enzymatic Recalitrance as Indicated by the Arabidopsis Mutant tbl29. <i>Molecular Plant</i>, 6, 1373-1375. YU, L., LYCZAKOWSKI, J. J., PEREIRA, C. S., KOTAKE, T., YU, X., LI, A., MOGELSVANG, S., SKAF, M. S. & DUPREE, P. 2018. The patterned structure of galactoglucomannan suggests it may bind to cellulose in seed mucilage. <i>Plant Physiolo</i>		
 972-979. THOMAS, L. H., FORSYTH, V. T., MARTEL, A., GRILLO, I., ALTANER, C. M. & JARVIS, M. C. 2014. Structure and spacing of cellulose microfibrils in woody cell walls of dicots. <i>Cellulose</i>, 21, 3887-3895. THOMAS, L. H., FORSYTH, V. T., MARTEL, A., GRILLO, I., ALTANER, C. M. & JARVIS, M. C. 2015. Diffraction evidence for the structure of cellulose microfibrils in bamboo, a model for grass and cereal celluloses. <i>Bmc Plant Biology</i>, 15. TURNER, S. & KUMAR, M. 2017. Cellulose synthase complex organization and cellulose microfibril structure. <i>Philosophical Transactions of the Royal Society</i> <i>A</i>, 376. TURNER, S. R. & SOMERVILLE, C. R. 1997. Collapsed xylem phenotype of Arabidopsis identifies mutants deficient in cellulose deposition in the secondary cell wall. <i>Plant Cell</i>, 9, 689-701. VANHOLME, R., DEMEDTS, B., MORREEL, K., RALPH, J., BOERJAN, W. 2010. Lignin biosynthesis and structure. <i>Plant Physiology</i>, 132, 1781-1789. VANHOLME, R., STORME, V., VANHOLME, B., SUNDIN, L., CHRISTENSEN, J. H., GOEMINNE, G., HALPIN, C., ROHDE, A., MORREEL, K. & BOERJAN, W. 2012. A Systems Biology View of Responses to Lignin Biosynthesis Perturbations in Arabidopsis. <i>Plant Cell</i>, 24, 3506-3529. WHITNEY, S. E. C., BRIGHAM, J. E., DARKE, A. H., REID, J. S. G. & GIDLEY, M. J. 1998. Structural aspects of the interaction of mannan-based polysaccharides with bacterial cellulose. <i>Carbohydrate Research</i>, 307, 299309. XIONG, G., CHENG, K. & PAULY, M. Xylan O-Acetylation Impacts Xylem Development and Enzymatic Recalcitrance as Indicated by the Arabidopsis Mutant tbl29. <i>Molecular Plant</i>, 6, 1373-1375. YU, L., LYCZAKOWSKI, J. J., PEREIRA, C. S., KOTAKE, T., YU, X., LI, A., MOGELSVANG, S., SKAF, M. S. & DUPREE, P. 2018. The patterned structure of galactoglucomannan suggests it may bind to cellulose in seed mucilage. <i>Plant Physiology</i>, 178, 1011-1026. ZHANG, X. Y., DOMINGUEZ, P. G., KUMAR, M., BYGDEL		
 THOMAS, L. H., FORSYTH, V. T., MARTEL, A., GRILLO, I., ALTANER, C. M. & JARVIS, M. C. 2014. Structure and spacing of cellulose microfibrils in woody cell walls of dicots. <i>Cellulose</i>, 21, 3887-3895. THOMAS, L. H., FORSYTH, V. T., MARTEL, A., GRILLO, I., ALTANER, C. M. & JARVIS, M. C. 2015. Diffraction evidence for the structure of cellulose microfibrils in bamboo, a model for grass and cereal celluloses. <i>Bmc Plant Biology</i>, 15. TURNER, S. & KUMAR, M. 2017. Cellulose synthase complex organization and cellulose microfibril structure. <i>Philosophical Transactions of the Royal Society</i> <i>A</i>, 376. TURNER, S. R. & SOMERVILLE, C. R. 1997. Collapsed xylem phenotype of Arabidopsis identifies mutants deficient in cellulose deposition in the secondary cell wall. <i>Plant Cell</i>, 9, 689-701. VANHOLME, R., DEMEDTS, B., MORREEL, K., RALPH, J., BOERJAN, W. 2010. Lignin biosynthesis and structure. <i>Plant Physiology</i>, 132, 1781-1789. VANHOLME, R., STORME, V., VANHOLME, B., SUNDIN, L., CHRISTENSEN, J. H., GOEMINNE, G., HALPIN, C., ROHDE, A., MORREEL, K. & BOERJAN, W. 2012. A Systems Biology View of Responses to Lignin Biosynthesis Perturbations in Arabidopsis. <i>Plant Cell</i>, 24, 3506-3529. WHITNEY, S. E. C., BRIGHAM, J. E., DARKE, A. H., REID, J. S. G. & GIDLEY, M. J. 1998. Structural aspects of the interaction of mannan-based polysaccharides with bacterial cellulose. <i>Carbohydrate Research</i>, 307, 299309. XIONG, G., CHENG, K. & PAULY, M. Xylan O-Acetylation Impacts Xylem Development and Enzymatic Recalcitrance as Indicated by the Arabidopsis Mutant tbl29. <i>Molecular Plant</i>, 6, 1373-1375. YU, L., LYCZAKOWSKI, J. J., PEREIRA, C. S., KOTAKE, T., YU, X., LI, A., MOGELSVANG, S., SKAF, M. S. & DUPREE, P. 2018. The patterned structure of galactoglucomannan suggests it may bind to cellulose in seed mucilage. <i>Plant Physiology</i>, 178, 1011-1026. ZHANG, T., ZHENG, Y. Z. & COSGROVE, D. J. 2016. Spatial organization of		
 JARVIS, M. C. 2014. Structure and spacing of cellulose microfibrils in woody cell walls of dicots. <i>Cellulose</i>, 21, 3887-3895. THOMAS, L. H., FORSYTH, V. T., MARTEL, A., GRILLO, I., ALTANER, C. M. & JARVIS, M. C. 2015. Diffraction evidence for the structure of cellulose microfibrils in bamboo, a model for grass and cereal celluloses. <i>Bmc Plant Biology</i>, 15. TURNER, S. & KUMAR, M. 2017. Cellulose synthase complex organization and cellulose microfibril structure. <i>Philosophical Transactions of the Royal Society</i> <i>A</i>, 376. TURNER, S. R. & SOMERVILLE, C. R. 1997. Collapsed xylem phenotype of Arabidopsis identifies mutants deficient in cellulose deposition in the secondary cell wall. <i>Plant Cell</i>, 9, 689-701. VANHOLME, R., DEMEDTS, B., MORREEL, K., RALPH, J., BOERJAN, W. 2010. Lignin biosynthesis and structure. <i>Plant Physiology</i>, 132, 1781-1789. VANHOLME, R., STORME, V., VANHOLME, B., SUNDIN, L., CHRISTENSEN, J. H., GCEMINNE, G., HALPIN, C., ROHDE, A., MORREEL, K. & BOERJAN, W. 2012. A Systems Biology View of Responses to Lignin Biosynthesis Perturbations in Arabidopsis. <i>Plant Cell</i>, 24, 3506-3529. WHITNEY, S. E. C., BRIGHAM, J. E., DARKE, A. H., REID, J. S. G. & GIDLEY, M. J. 1998. Structural aspects of the interaction of mannan-based polysaccharides with bacterial cellulose. <i>Carbohydrate Research</i>, 307, 299309. XIONG, G., CHENG, K. & PAULY, M. Xylan O-Acetylation Impacts Xylem Development and Enzymatic Recalcitrance as Indicated by the Arabidopsis Mutant tb129. <i>Molecular Plant</i>, 6, 1373-1375. YU, L., LYCZAKOWSKI, J. J., PEREIRA, C. S., KOTAKE, T., YU, X., LI, A., MOGELSVANG, S., SKAF, M. S. & DUPREE, P. 2018. The patterned structure of galactoglucomannan suggests it may bind to cellulose in seed mucilage. <i>Plant Physiology</i>, 178, 1011-1026. ZHANG, X. Y., DOMINGUEZ, P. G., KUMAR, M., BYGDELL, J., MIROSHNICHENKO, S., SUNDBERG, B., WINGSLE, G. & NIITTYLA, T. 2018. Cellulose Synthase S		
 cell walls of dicots. <i>Cellulose</i>, 21, 3887-3895. THOMAS, L. H., FORSYTH, V. T., MARTEL, A., GRILLO, I., ALTANER, C. M. & JARVIS, M. C. 2015. Diffraction evidence for the structure of cellulose microfibrils in bamboo, a model for grass and cereal celluloses. <i>Bmc Plant Biology</i>, 15. TURNER, S. & KUMAR, M. 2017. Cellulose synthase complex organization and cellulose microfibril structure. <i>Philosophical Transactions of the Royal Society</i> <i>A</i>, 376. TURNER, S. R. & SOMERVILLE, C. R. 1997. Collapsed xylem phenotype of Arabidopsis identifies mutants deficient in cellulose deposition in the secondary cell wall. <i>Plant Cell</i>, 9, 689-701. VANHOLME, R., DEMEDTS, B., MORREEL, K., RALPH, J., BOERJAN, W. 2010. Lignin biosynthesis and structure. <i>Plant Physiology</i>, 132, 1781-1789. VANHOLME, R., STORME, V., VANHOLME, B., SUNDIN, L., CHRISTENSEN, J. H., GOEMINNE, G., HALPIN, C., ROHDE, A., MORREEL, K. & BOERJAN, W. 2012. A Systems Biology View of Responses to Lignin Biosynthesis Perturbations in Arabidopsis. <i>Plant Cell</i>, 24, 3506-3529. WHITNEY, S. E. C., BRIGHAM, J. E., DARKE, A. H., REID, J. S. G. & GIDLEY, M. J. 1998. Structural aspects of the interaction of mannan-based polysaccharides with bacterial cellulose. <i>Carbohydrate Research</i>, 307, 299309. XIONG, G., CHENG, K. & PAULY, M. Xylan O-Acetylation Impacts Xylem Development and Enzymatic Recalcitrance as Indicated by the Arabidopsis Mutant tbl29. <i>Molecular Plant</i>, 6, 1373-1375. YU, L., LYCZAKOWSKI, J. J., PEREIRA, C. S., KOTAKE, T., YU, X., LI, A., MOGELSVANG, S., SKAF, M. S. & DUPREE, P. 2018. The patterned structure of galactoglucomannan suggests it may bind to cellulose in seed mucilage. <i>Plant Physiology</i>, 178, 1011-1026. ZHANG, T., ZHENG, Y. Z. & COSGROVE, D. J. 2016. Spatial organization of cellulose microfibrils and matrix polysaccharides in primary plant cell walls as imaged by multichannel atomic force microscopy. <i>Plant Journal</i>, 85		
 THOMAS, L. H., FORSYTH, V. T., MARTEL, A., GRILLO, I., ALTANER, C. M. & JARVIS, M. C. 2015. Diffraction evidence for the structure of cellulose microfibrils in bamboo, a model for grass and cereal celluloses. <i>Bmc Plant Biology</i>, 15. TURNER, S. & KUMAR, M. 2017. Cellulose synthase complex organization and cellulose microfibril structure. <i>Philosophical Transactions of the Royal Society</i> <i>A</i>, 376. TURNER, S. R. & SOMERVILLE, C. R. 1997. Collapsed xylem phenotype of Arabidopsis identifies mutants deficient in cellulose deposition in the secondary cell wall. <i>Plant Cell</i>, 9, 689-701. VANHOLME, R., DEMEDTS, B., MORREEL, K., RALPH, J., BOERJAN, W. 2010. Lignin biosynthesis and structure. <i>Plant Physiology</i>, 132, 1781-1789. VANHOLME, R., STORME, V., VANHOLME, B., SUNDIN, L., CHRISTENSEN, J. H., GOEMINNE, G., HALPIN, C., ROHDE, A., MORREEL, K. & BOERJAN, W. 2012. A Systems Biology View of Responses to Lignin Biosynthesis Perturbations in Arabidopsis. <i>Plant Cell</i>, 24, 3506-3529. WHITNEY, S. E. C., BRIGHAM, J. E., DARKE, A. H., REID, J. S. G. & GIDLEY, M. J. 1998. Structural aspects of the interaction of mannan-based polysaccharides with bacterial cellulose. <i>Carbohydrate Research</i>, 307, 299309. XIONG, G., CHENG, K. & PAULY, M. Xylan O-Acetylation Impacts Xylem Development and Enzymatic Recalcitrance as Indicated by the Arabidopsis Mutant tbl29. <i>Molecular Plant</i>, 6, 1373-1375. YU, L., LYCZAKOWSKI, J. J., PEREIRA, C. S., KOTAKE, T., YU, X., LI, A., MOGELSVANG, S., SKAF, M. S. & DUPREE, P. 2018. The patterned structure of galactoglucomannan suggests it may bind to cellulose in seed mucilage. <i>Plant Physiology</i>, 178, 1011-1026. ZHANG, T., ZHENG, Y. Z. & COSGROVE, D. J. 2016. Spatial organization of cellulose microfibrils and matrix polysaccharides in primary plant cell walls as imaged by multichannel atomic force microscopy. <i>Plant Journal</i>, 85, 179-192. ZHANG, X. Y., DOMINGUEZ, P. G., KUMAR,		
 JARVIS, M. C. 2015. Diffraction evidence for the structure of cellulose microfibrils in bamboo, a model for grass and cereal celluloses. <i>Bmc Plant</i> <i>Biology</i>, 15. TURNER, S. & KUMAR, M. 2017. Cellulose synthase complex organization and cellulose microfibril structure. <i>Philosophical Transactions of the Royal Society</i> <i>A</i>, 376. TURNER, S. R. & SOMERVILLE, C. R. 1997. Collapsed xylem phenotype of Arabidopsis identifies mutants deficient in cellulose deposition in the secondary cell wall. <i>Plant Cell</i>, 9, 689-701. VANHOLME, R., DEMEDTS, B., MORREEL, K., RALPH, J., BOERJAN, W. 2010. Lignin biosynthesis and structure. <i>Plant Physiology</i>, 132, 1781-1789. VANHOLME, R., STORME, V., VANHOLME, B., SUNDIN, L., CHRISTENSEN, J. H., GOEMINNE, G., HALPIN, C., ROHDE, A., MORREEL, K. & BOERJAN, W. 2012. A Systems Biology View of Responses to Lignin Biosynthesis Perturbations in Arabidopsis. <i>Plant Cell</i>, 24, 3506-3529. WHITNEY, S. E. C., BRIGHAM, J. E., DARKE, A. H., REID, J. S. G. & GIDLEY, M. J. 1998. Structural aspects of the interaction of mannan-based polysaccharides with bacterial cellulose. <i>Carbohydrate Research</i>, 307, 299309. XIONG, G., CHENG, K. & PAULY, M. Xylan O-Acetylation Impacts Xylem Development and Enzymatic Recalcitrance as Indicated by the Arabidopsis Mutant tbl29. <i>Molecular Plant</i>, 6, 1373-1375. YU, L., LYCZAKOWSKI, J. J., PEREIRA, C. S., KOTAKE, T., YU, X., LI, A., MOGELSVANG, S., SKAF, M. S. & DUPREE, P. 2018. The patterned structure of galactoglucomannan suggests it may bind to cellulose in seed mucilage. <i>Plant Physiology</i>, 178, 1011-1026. ZHANG, T., ZHENG, Y. Z. & COSGROVE, D. J. 2016. Spatial organization of cellulose microfibrils and matrix polysaccharides in primary plant cell walls as imaged by multichannel atomic force microscopy. <i>Plant Journal</i>, 85, 179-192. ZHANG, X. Y., DOMINGUEZ, P. G., KUMAR, M., BYGDELL, J., MIROSHNICHENKO, S., SUNDBERG, B., WINGSLE, G. & NIITT		
 microfibrils in bamboo, a model for grass and cereal celluloses. <i>Bmc Plant</i> <i>Biology</i>, 15. TURNER, S. & KUMAR, M. 2017. Cellulose synthase complex organization and cellulose microfibril structure. <i>Philosophical Transactions of the Royal Society</i> <i>A</i>, 376. TURNER, S. R. & SOMERVILLE, C. R. 1997. Collapsed xylem phenotype of Arabidopsis identifies mutants deficient in cellulose deposition in the secondary cell wall. <i>Plant Cell</i>, 9, 689-701. VANHOLME, R., DEMEDTS, B., MORREEL, K., RALPH, J., BOERJAN, W. 2010. Lignin biosynthesis and structure. <i>Plant Physiology</i>, 132, 1781-1789. VANHOLME, R., STORME, V., VANHOLME, B., SUNDIN, L., CHRISTENSEN, J. H., GOEMINNE, G., HALPIN, C., ROHDE, A., MORREEL, K. & BOERJAN, W. 2012. A Systems Biology View of Responses to Lignin Biosynthesis Perturbations in Arabidopsis. <i>Plant Cell</i>, 24, 3506-3529. WHITNEY, S. E. C., BRIGHAM, J. E., DARKE, A. H., REID, J. S. G. & GIDLEY, M. J. 1998. Structural aspects of the interaction of mannan-based polysaccharides with bacterial cellulose. <i>Carbohydrate Research</i>, 307, 299309. XIONG, G., CHENG, K. & PAULY, M. Xylan O-Acetylation Impacts Xylem Development and Enzymatic Recalcitrance as Indicated by the Arabidopsis Mutant tbl29. <i>Molecular Plant</i>, 6, 1373-1375. YU, L., LYCZAKOWSKI, J. J., PEREIRA, C. S., KOTAKE, T., YU, X., LI, A., MOGELSVANG, S., SKAF, M. S. & DUPREE, P. 2018. The patterned structure of galactoglucomannan suggests it may bind to cellulose in seed mucilage. <i>Plant Physiology</i>, 178, 1011-1026. ZHANG, T., ZHENG, Y. Z. & COSGROVE, D. J. 2016. Spatial organization of cellulose microfibrils and matrix polysaccharides in primary plant cell walls as imaged by multichannel atomic force microscopy. <i>Plant Journal</i>, 85, 179-192. ZHANG, X. Y., DOMINGUEZ, P. G., KUMAR, M., BYGDELL, J., MIROSHNICHENKO, S., SUNDBERG, B., WINGSLE, G. & NIITTYLA, T. 2018. Cellulose Synthase Stoichiometry in Aspen Differs from Ara		
 Biology, 15. TURNER, S. & KUMAR, M. 2017. Cellulose synthase complex organization and cellulose microfibril structure. <i>Philosophical Transactions of the Royal Society</i> <i>A</i>, 376. TURNER, S. R. & SOMERVILLE, C. R. 1997. Collapsed xylem phenotype of Arabidopsis identifies mutants deficient in cellulose deposition in the secondary cell wall. <i>Plant Cell</i>, 9, 689-701. VANHOLME, R., DEMEDTS, B., MORREEL, K., RALPH, J., BOERJAN, W. 2010. Lignin biosynthesis and structure. <i>Plant Physiology</i>, 132, 1781-1789. VANHOLME, R., STORME, V., VANHOLME, B., SUNDIN, L., CHRISTENSEN, J. H., GOEMINNE, G., HALPIN, C., ROHDE, A., MORREEL, K. & BOERJAN, W. 2012. A Systems Biology View of Responses to Lignin Biosynthesis Perturbations in Arabidopsis. <i>Plant Cell</i>, 24, 3506-3529. WHITNEY, S. E. C., BRIGHAM, J. E., DARKE, A. H., REID, J. S. G. & GIDLEY, M. J. 1998. Structural aspects of the interaction of mannan-based polysaccharides with bacterial cellulose. <i>Carbohydrate Research</i>, 307, 299309. XIONG, G., CHENG, K. & PAULY, M. Xylan O-Acetylation Impacts Xylem Development and Enzymatic Recalcitrance as Indicated by the Arabidopsis Mutant tbl29. <i>Molecular Plant</i>, 6, 1373-1375. YU, L., LYCZAKOWSKI, J. J., PEREIRA, C. S., KOTAKE, T., YU, X., LI, A., MOGELSVANG, S., SKAF, M. S. & DUPREE, P. 2018. The patterned structure of galactoglucomannan suggests it may bind to cellulose in seed mucilage. <i>Plant Physiology</i>, 178, 1011-1026. ZHANG, T., ZHENG, Y. Z. & COSGROVE, D. J. 2016. Spatial organization of cellulose microfibrils and matrix polysaccharides in primary plant cell walls as imaged by multichannel atomic force microscopy. <i>Plant Journal</i>, 85, 179-192. ZHANG, X. Y., DOMINGUEZ, P. G., KUMAR, M., BYGDELL, J., MIROSHNICHENKO, S., SUNDBERG, B., WINGSLE, G. & NIITTYLA, T. 2018. Cellulose Synthase Stoichiometry in Aspen Differs from Arabidopsis 		
 TURNER, S. & KUMAR, M. 2017. Cellulose synthase complex organization and cellulose microfibril structure. <i>Philosophical Transactions of the Royal Society</i> <i>A</i>, 376. TURNER, S. R. & SOMERVILLE, C. R. 1997. Collapsed xylem phenotype of Arabidopsis identifies mutants deficient in cellulose deposition in the secondary cell wall. <i>Plant Cell</i>, 9, 689-701. VANHOLME, R., DEMEDTS, B., MORREEL, K., RALPH, J., BOERJAN, W. 2010. Lignin biosynthesis and structure. <i>Plant Physiology</i>, 132, 1781-1789. VANHOLME, R., STORME, V., VANHOLME, B., SUNDIN, L., CHRISTENSEN, J. H., GOEMINNE, G., HALPIN, C., ROHDE, A., MORREEL, K. & BOERJAN, W. 2012. A Systems Biology View of Responses to Lignin Biosynthesis Perturbations in Arabidopsis. <i>Plant Cell</i>, 24, 3506-3529. WHITNEY, S. E. C., BRIGHAM, J. E., DARKE, A. H., REID, J. S. G. & GIDLEY, M. J. 1998. Structural aspects of the interaction of mannan-based polysaccharides with bacterial cellulose. <i>Carbohydrate Research</i>, 307, 299309. XIONG, G., CHENG, K. & PAULY, M. Xylan O-Acetylation Impacts Xylem Development and Enzymatic Recalcitrance as Indicated by the Arabidopsis Mutant tbl29. <i>Molecular Plant</i>, 6, 1373-1375. YU, L., LYCZAKOWSKI, J. J., PEREIRA, C. S., KOTAKE, T., YU, X., LI, A., MOGELSVANG, S., SKAF, M. S. & DUPREE, P. 2018. The patterned structure of galactoglucomannan suggests it may bind to cellulose in seed mucilage. <i>Plant Physiology</i>, 178, 1011-1026. ZHANG, T., ZHENG, Y. Z. & COSGROVE, D. J. 2016. Spatial organization of cellulose microfibrils and matrix polysaccharides in primary plant cell walls as imaged by multichannel atomic force microscopy. <i>Plant Journal</i>, 85, 179-192. ZHANG, X. Y., DOMINGUEZ, P. G., KUMAR, M., BYGDELL, J., MIROSHNICHENKO, S., SUNDBERG, B., WINGSLE, G. & NIITTYLA, T. 2018. Cellulose Synthase Stoichiometry in Aspen Differs from Arabidopsis 		
 cellulose microfibril structure. <i>Philosophical Transactions of the Royal Society</i> <i>A</i>, 376. TURNER, S. R. & SOMERVILLE, C. R. 1997. Collapsed xylem phenotype of Arabidopsis identifies mutants deficient in cellulose deposition in the secondary cell wall. <i>Plant Cell</i>, 9, 689-701. VANHOLME, R., DEMEDTS, B., MORREEL, K., RALPH, J., BOERJAN, W. 2010. Lignin biosynthesis and structure. <i>Plant Physiology</i>, 132, 1781-1789. VANHOLME, R., STORME, V., VANHOLME, B., SUNDIN, L., CHRISTENSEN, J. H., GOEMINNE, G., HALPIN, C., ROHDE, A., MORREEL, K. & BOERJAN, W. 2012. A Systems Biology View of Responses to Lignin Biosynthesis Perturbations in Arabidopsis. <i>Plant Cell</i>, 24, 3506-3529. WHITNEY, S. E. C., BRIGHAM, J. E., DARKE, A. H., REID, J. S. G. & GIDLEY, M. J. 1998. Structural aspects of the interaction of mannan-based polysaccharides with bacterial cellulose. <i>Carbohydrate Research</i>, 307, 299309. XIONG, G., CHENG, K. & PAULY, M. Xylan O-Acetylation Impacts Xylem Development and Enzymatic Recalcitrance as Indicated by the Arabidopsis Mutant tbl29. <i>Molecular Plant</i>, 6, 1373-1375. YU, L., LYCZAKOWSKI, J. J., PEREIRA, C. S., KOTAKE, T., YU, X., LI, A., MOGELSVANG, S., SKAF, M. S. & DUPREE, P. 2018. The patterned structure of galactoglucomannan suggests it may bind to cellulose in seed mucilage. <i>Plant Physiology</i>, 178, 1011-1026. ZHANG, T., ZHENG, Y. Z. & COSGROVE, D. J. 2016. Spatial organization of cellulose microfibrils and matrix polysaccharides in primary plant cell walls as imaged by multichannel atomic force microscopy. <i>Plant Journal</i>, 85, 179-192. ZHANG, X. Y., DOMINGUEZ, P. G., KUMAR, M., BYGDELL, J., MIROSHNICHENKO, S., SUNDBERG, B., WINGSLE, G. & NIITTYLA, T. 2018. Cellulose Synthase Stoichiometry in Aspen Differs from Arabidopsis 		
 A, 376. TURNER, S. R. & SOMERVILLE, C. R. 1997. Collapsed xylem phenotype of Arabidopsis identifies mutants deficient in cellulose deposition in the secondary cell wall. <i>Plant Cell</i>, 9, 689-701. VANHOLME, R., DEMEDTS, B., MORREEL, K., RALPH, J., BOERJAN, W. 2010. Lignin biosynthesis and structure. <i>Plant Physiology</i>, 132, 1781-1789. VANHOLME, R., STORME, V., VANHOLME, B., SUNDIN, L., CHRISTENSEN, J. H., GOEMINNE, G., HALPIN, C., ROHDE, A., MORREEL, K. & BOERJAN, W. 2012. A Systems Biology View of Responses to Lignin Biosynthesis Perturbations in Arabidopsis. <i>Plant Cell</i>, 24, 3506-3529. WHITNEY, S. E. C., BRIGHAM, J. E., DARKE, A. H., REID, J. S. G. & GIDLEY, M. J. 1998. Structural aspects of the interaction of manan-based polysaccharides with bacterial cellulose. <i>Carbohydrate Research</i>, 307, 299309. XIONG, G., CHENG, K. & PAULY, M. Xylan O-Acetylation Impacts Xylem Development and Enzymatic Recalcitrance as Indicated by the Arabidopsis Mutant tbl29. <i>Molecular Plant</i>, 6, 1373-1375. YU, L., LYCZAKOWSKI, J. J., PEREIRA, C. S., KOTAKE, T., YU, X., LI, A., MOGELSVANG, S., SKAF, M. S. & DUPREE, P. 2018. The patterned structure of galactoglucomannan suggests it may bind to cellulose in seed mucilage. <i>Plant Physiology</i>, 178, 1011-1026. ZHANG, T., ZHENG, Y. Z. & COSGROVE, D. J. 2016. Spatial organization of cellulose microfibrils and matrix polysaccharides in primary plant cell walls as imaged by multichannel atomic force microscopy. <i>Plant Journal</i>, 85, 179-192. ZHANG, X. Y., DOMINGUEZ, P. G., KUMAR, M., BYGDELL, J., MIROSHNICHENKO, S., SUNDBERG, B., WINGSLE, G. & NIITTYLA, T. 2018. Cellulose Synthase Stoichiometry in Aspen Differs from Arabidopsis 		
 TURNER, S. R. & SOMERVILLE, C. R. 1997. Collapsed xylem phenotype of Arabidopsis identifies mutants deficient in cellulose deposition in the secondary cell wall. <i>Plant Cell</i>, 9, 689-701. VANHOLME, R., DEMEDTS, B., MORREEL, K., RALPH, J., BOERJAN, W. 2010. Lignin biosynthesis and structure. <i>Plant Physiology</i>, 132, 1781-1789. VANHOLME, R., STORME, V., VANHOLME, B., SUNDIN, L., CHRISTENSEN, J. H., GOEMINNE, G., HALPIN, C., ROHDE, A., MORREEL, K. & BOERJAN, W. 2012. A Systems Biology View of Responses to Lignin Biosynthesis Perturbations in Arabidopsis. <i>Plant Cell</i>, 24, 3506-3529. WHITNEY, S. E. C., BRIGHAM, J. E., DARKE, A. H., REID, J. S. G. & GIDLEY, M. J. 1998. Structural aspects of the interaction of mannan-based polysaccharides with bacterial cellulose. <i>Carbohydrate Research</i>, 307, 299309. XIONG, G., CHENG, K. & PAULY, M. Xylan O-Acetylation Impacts Xylem Development and Enzymatic Recalcitrance as Indicated by the Arabidopsis Mutant tbl29. <i>Molecular Plant</i>, 6, 1373-1375. YU, L., LYCZAKOWSKI, J. J., PEREIRA, C. S., KOTAKE, T., YU, X., LI, A., MOGELSVANG, S., SKAF, M. S. & DUPREE, P. 2018. The patterned structure of galactoglucomannan suggests it may bind to cellulose in seed mucilage. <i>Plant Physiology</i>, 178, 1011-1026. ZHANG, T., ZHENG, Y. Z. & COSGROVE, D. J. 2016. Spatial organization of cellulose microfibrils and matrix polysaccharides in primary plant cell walls as imaged by multichannel atomic force microscopy. <i>Plant Journal</i>, 85, 179-192. ZHANG, X. Y., DOMINGUEZ, P. G., KUMAR, M., BYGDELL, J., MIROSHNICHENKO, S., SUNDBERG, B., WINGSLE, G. & NIITTYLA, T. 2018. Cellulose Synthase Stoichiometry in Aspen Differs from Arabidopsis 		
 Arabidopsis identifies mutants deficient in cellulose deposition in the secondary cell wall. <i>Plant Cell</i>, 9, 689-701. VANHOLME, R., DEMEDTS, B., MORREEL, K., RALPH, J., BOERJAN, W. 2010. Lignin biosynthesis and structure. <i>Plant Physiology</i>, 132, 1781-1789. VANHOLME, R., STORME, V., VANHOLME, B., SUNDIN, L., CHRISTENSEN, J. H., GOEMINNE, G., HALPIN, C., ROHDE, A., MORREEL, K. & BOERJAN, W. 2012. A Systems Biology View of Responses to Lignin Biosynthesis Perturbations in Arabidopsis. <i>Plant Cell</i>, 24, 3506-3529. WHITNEY, S. E. C., BRIGHAM, J. E., DARKE, A. H., REID, J. S. G. & GIDLEY, M. J. 1998. Structural aspects of the interaction of mannan-based polysaccharides with bacterial cellulose. <i>Carbohydrate Research</i>, 307, 299309. XIONG, G., CHENG, K. & PAULY, M. Xylan O-Acetylation Impacts Xylem Development and Enzymatic Recalcitrance as Indicated by the Arabidopsis Mutant tbl29. <i>Molecular Plant</i>, 6, 1373-1375. YU, L., LYCZAKOWSKI, J. J., PEREIRA, C. S., KOTAKE, T., YU, X., LI, A., MOGELSVANG, S., SKAF, M. S. & DUPREE, P. 2018. The patterned structure of galactoglucomannan suggests it may bind to cellulose in seed mucilage. <i>Plant Physiology</i>, 178, 1011-1026. ZHANG, T., ZHENG, Y. Z. & COSGROVE, D. J. 2016. Spatial organization of cellulose microfibrils and matrix polysaccharides in primary plant cell walls as imaged by multichannel atomic force microscopy. <i>Plant Journal</i>, 85, 179-192. ZHANG, X. Y., DOMINGUEZ, P. G., KUMAR, M., BYGDELL, J., MIROSHNICHENKO, S., SUNDBERG, B., WINGSLE, G. & NIITTYLA, T. 2018. Cellulose Synthase Stoichiometry in Aspen Differs from Arabidopsis 		
 secondary cell wall. <i>Plant Cell</i>, 9, 689-701. VANHOLME, R., DEMEDTS, B., MORREEL, K., RALPH, J., BOERJAN, W. 2010. Lignin biosynthesis and structure. <i>Plant Physiology</i>, 132, 1781-1789. VANHOLME, R., STORME, V., VANHOLME, B., SUNDIN, L., CHRISTENSEN, J. H., GOEMINNE, G., HALPIN, C., ROHDE, A., MORREEL, K. & BOERJAN, W. 2012. A Systems Biology View of Responses to Lignin Biosynthesis Perturbations in Arabidopsis. <i>Plant Cell</i>, 24, 3506-3529. WHITNEY, S. E. C., BRIGHAM, J. E., DARKE, A. H., REID, J. S. G. & GIDLEY, M. J. 1998. Structural aspects of the interaction of mannan-based polysaccharides with bacterial cellulose. <i>Carbohydrate Research</i>, 307, 299309. XIONG, G., CHENG, K. & PAULY, M. Xylan O-Acetylation Impacts Xylem Development and Enzymatic Recalcitrance as Indicated by the Arabidopsis Mutant tbl29. <i>Molecular Plant</i>, 6, 1373-1375. YU, L., LYCZAKOWSKI, J. J., PEREIRA, C. S., KOTAKE, T., YU, X., LI, A., MOGELSVANG, S., SKAF, M. S. & DUPREE, P. 2018. The patterned structure of galactoglucomannan suggests it may bind to cellulose in seed mucilage. <i>Plant Physiology</i>, 178, 1011-1026. ZHANG, T., ZHENG, Y. Z. & COSGROVE, D. J. 2016. Spatial organization of cellulose microfibrils and matrix polysaccharides in primary plant cell walls as imaged by multichannel atomic force microscopy. <i>Plant Journal</i>, 85, 179-192. ZHANG, X. Y., DOMINGUEZ, P. G., KUMAR, M., BYGDELL, J., MIROSHNICHENKO, S., SUNDBERG, B., WINGSLE, G. & NIITTYLA, T. 2018. Cellulose Synthase Stoichiometry in Aspen Differs from Arabidopsis 		
 VANHOLME, R., DEMEDTS, B., MORREEL, K., RALPH, J., BOERJAN, W. 2010. Lignin biosynthesis and structure. <i>Plant Physiology</i>, 132, 1781-1789. VANHOLME, R., STORME, V., VANHOLME, B., SUNDIN, L., CHRISTENSEN, J. H., GOEMINNE, G., HALPIN, C., ROHDE, A., MORREEL, K. & BOERJAN, W. 2012. A Systems Biology View of Responses to Lignin Biosynthesis Perturbations in Arabidopsis. <i>Plant Cell</i>, 24, 3506-3529. WHITNEY, S. E. C., BRIGHAM, J. E., DARKE, A. H., REID, J. S. G. & GIDLEY, M. J. 1998. Structural aspects of the interaction of mannan-based polysaccharides with bacterial cellulose. <i>Carbohydrate Research</i>, 307, 299309. XIONG, G., CHENG, K. & PAULY, M. Xylan O-Acetylation Impacts Xylem Development and Enzymatic Recalcitrance as Indicated by the Arabidopsis Mutant tbl29. <i>Molecular Plant</i>, 6, 1373-1375. YU, L., LYCZAKOWSKI, J. J., PEREIRA, C. S., KOTAKE, T., YU, X., LI, A., MOGELSVANG, S., SKAF, M. S. & DUPREE, P. 2018. The patterned structure of galactoglucomannan suggests it may bind to cellulose in seed mucilage. <i>Plant Physiology</i>, 178, 1011-1026. ZHANG, T., ZHENG, Y. Z. & COSGROVE, D. J. 2016. Spatial organization of cellulose microfibrils and matrix polysaccharides in primary plant cell walls as imaged by multichannel atomic force microscopy. <i>Plant Journal</i>, 85, 179-192. ZHANG, X. Y., DOMINGUEZ, P. G., KUMAR, M., BYGDELL, J., MIROSHNICHENKO, S., SUNDBERG, B., WINGSLE, G. & NIITTYLA, T. 2018. Cellulose Synthase Stoichiometry in Aspen Differs from Arabidopsis 		•
 Lignin biosynthesis and structure. <i>Plant Physiology</i>, 132, 1781-1789. VANHOLME, R., STORME, V., VANHOLME, B., SUNDIN, L., CHRISTENSEN, J. H., GOEMINNE, G., HALPIN, C., ROHDE, A., MORREEL, K. & BOERJAN, W. 2012. A Systems Biology View of Responses to Lignin Biosynthesis Perturbations in Arabidopsis. <i>Plant Cell</i>, 24, 3506-3529. WHITNEY, S. E. C., BRIGHAM, J. E., DARKE, A. H., REID, J. S. G. & GIDLEY, M. J. 1998. Structural aspects of the interaction of mannan-based polysaccharides with bacterial cellulose. <i>Carbohydrate Research</i>, 307, 299309. XIONG, G., CHENG, K. & PAULY, M. Xylan O-Acetylation Impacts Xylem Development and Enzymatic Recalcitrance as Indicated by the Arabidopsis Mutant tbl29. <i>Molecular Plant</i>, 6, 1373-1375. YU, L., LYCZAKOWSKI, J. J., PEREIRA, C. S., KOTAKE, T., YU, X., LI, A., MOGELSVANG, S., SKAF, M. S. & DUPREE, P. 2018. The patterned structure of galactoglucomannan suggests it may bind to cellulose in seed mucilage. <i>Plant Physiology</i>, 178, 1011-1026. ZHANG, T., ZHENG, Y. Z. & COSGROVE, D. J. 2016. Spatial organization of cellulose microfibrils and matrix polysaccharides in primary plant cell walls as imaged by multichannel atomic force microscopy. <i>Plant Journal</i>, 85, 179-192. ZHANG, X. Y., DOMINGUEZ, P. G., KUMAR, M., BYGDELL, J., MIROSHNICHENKO, S., SUNDBERG, B., WINGSLE, G. & NIITTYLA, T. 2018. Cellulose Synthase Stoichiometry in Aspen Differs from Arabidopsis 		
 VANHOLME, R., STORME, V., VANHOLME, B., SUNDIN, L., CHRISTENSEN, J. H., GOEMINNE, G., HALPIN, C., ROHDE, A., MORREEL, K. & BOERJAN, W. 2012. A Systems Biology View of Responses to Lignin Biosynthesis Perturbations in Arabidopsis. <i>Plant Cell</i>, 24, 3506-3529. WHITNEY, S. E. C., BRIGHAM, J. E., DARKE, A. H., REID, J. S. G. & GIDLEY, M. J. 1998. Structural aspects of the interaction of mannan-based polysaccharides with bacterial cellulose. <i>Carbohydrate Research</i>, 307, 299309. XIONG, G., CHENG, K. & PAULY, M. Xylan O-Acetylation Impacts Xylem Development and Enzymatic Recalcitrance as Indicated by the Arabidopsis Mutant tbl29. <i>Molecular Plant</i>, 6, 1373-1375. YU, L., LYCZAKOWSKI, J. J., PEREIRA, C. S., KOTAKE, T., YU, X., LI, A., MOGELSVANG, S., SKAF, M. S. & DUPREE, P. 2018. The patterned structure of galactoglucomannan suggests it may bind to cellulose in seed mucilage. <i>Plant Physiology</i>, 178, 1011-1026. ZHANG, T., ZHENG, Y. Z. & COSGROVE, D. J. 2016. Spatial organization of cellulose microfibrils and matrix polysaccharides in primary plant cell walls as imaged by multichannel atomic force microscopy. <i>Plant Journal</i>, 85, 179-192. ZHANG, X. Y., DOMINGUEZ, P. G., KUMAR, M., BYGDELL, J., MIROSHNICHENKO, S., SUNDBERG, B., WINGSLE, G. & NIITTYLA, T. 2018. Cellulose Synthase Stoichiometry in Aspen Differs from Arabidopsis 		
 GOEMINNE, G., HALPIN, C., ROHDE, A., MORREEL, K. & BOERJAN, W. 2012. A Systems Biology View of Responses to Lignin Biosynthesis Perturbations in Arabidopsis. <i>Plant Cell</i>, 24, 3506-3529. WHITNEY, S. E. C., BRIGHAM, J. E., DARKE, A. H., REID, J. S. G. & GIDLEY, M. J. 1998. Structural aspects of the interaction of mannan-based polysaccharides with bacterial cellulose. <i>Carbohydrate Research</i>, 307, 299309. XIONG, G., CHENG, K. & PAULY, M. Xylan O-Acetylation Impacts Xylem Development and Enzymatic Recalcitrance as Indicated by the Arabidopsis Mutant tbl29. <i>Molecular Plant</i>, 6, 1373-1375. YU, L., LYCZAKOWSKI, J. J., PEREIRA, C. S., KOTAKE, T., YU, X., LI, A., MOGELSVANG, S., SKAF, M. S. & DUPREE, P. 2018. The patterned structure of galactoglucomannan suggests it may bind to cellulose in seed mucilage. <i>Plant Physiology</i>, 178, 1011-1026. ZHANG, T., ZHENG, Y. Z. & COSGROVE, D. J. 2016. Spatial organization of cellulose microfibrils and matrix polysaccharides in primary plant cell walls as imaged by multichannel atomic force microscopy. <i>Plant Journal</i>, 85, 179-192. ZHANG, X. Y., DOMINGUEZ, P. G., KUMAR, M., BYGDELL, J., MIROSHNICHENKO, S., SUNDBERG, B., WINGSLE, G. & NIITTYLA, T. 2018. Cellulose Synthase Stoichiometry in Aspen Differs from Arabidopsis 		
 2012. A Systems Biology View of Responses to Lignin Biosynthesis Perturbations in Arabidopsis. <i>Plant Cell</i>, 24, 3506-3529. WHITNEY, S. E. C., BRIGHAM, J. E., DARKE, A. H., REID, J. S. G. & GIDLEY, M. J. 1998. Structural aspects of the interaction of mannan-based polysaccharides with bacterial cellulose. <i>Carbohydrate Research</i>, 307, 299309. XIONG, G., CHENG, K. & PAULY, M. Xylan O-Acetylation Impacts Xylem Development and Enzymatic Recalcitrance as Indicated by the Arabidopsis Mutant tbl29. <i>Molecular Plant</i>, 6, 1373-1375. YU, L., LYCZAKOWSKI, J. J., PEREIRA, C. S., KOTAKE, T., YU, X., LI, A., MOGELSVANG, S., SKAF, M. S. & DUPREE, P. 2018. The patterned structure of galactoglucomannan suggests it may bind to cellulose in seed mucilage. <i>Plant Physiology</i>, 178, 1011-1026. ZHANG, T., ZHENG, Y. Z. & COSGROVE, D. J. 2016. Spatial organization of cellulose microfibrils and matrix polysaccharides in primary plant cell walls as imaged by multichannel atomic force microscopy. <i>Plant Journal</i>, 85, 179-192. ZHANG, X. Y., DOMINGUEZ, P. G., KUMAR, M., BYGDELL, J., MIROSHNICHENKO, S., SUNDBERG, B., WINGSLE, G. & NIITTYLA, T. 2018. Cellulose Synthase Stoichiometry in Aspen Differs from Arabidopsis 		
 Perturbations in Arabidopsis. <i>Plant Cell</i>, 24, 3506-3529. WHITNEY, S. E. C., BRIGHAM, J. E., DARKE, A. H., REID, J. S. G. & GIDLEY, M. J. 1998. Structural aspects of the interaction of mannan-based polysaccharides with bacterial cellulose. <i>Carbohydrate Research</i>, 307, 299309. XIONG, G., CHENG, K. & PAULY, M. Xylan O-Acetylation Impacts Xylem Development and Enzymatic Recalcitrance as Indicated by the Arabidopsis Mutant tbl29. <i>Molecular Plant</i>, 6, 1373-1375. YU, L., LYCZAKOWSKI, J. J., PEREIRA, C. S., KOTAKE, T., YU, X., LI, A., MOGELSVANG, S., SKAF, M. S. & DUPREE, P. 2018. The patterned structure of galactoglucomannan suggests it may bind to cellulose in seed mucilage. <i>Plant Physiology</i>, 178, 1011-1026. ZHANG, T., ZHENG, Y. Z. & COSGROVE, D. J. 2016. Spatial organization of cellulose microfibrils and matrix polysaccharides in primary plant cell walls as imaged by multichannel atomic force microscopy. <i>Plant Journal</i>, 85, 179-192. ZHANG, X. Y., DOMINGUEZ, P. G., KUMAR, M., BYGDELL, J., MIROSHNICHENKO, S., SUNDBERG, B., WINGSLE, G. & NIITTYLA, T. 2018. Cellulose Synthase Stoichiometry in Aspen Differs from Arabidopsis 		
 WHITNEY, S. E. C., BRIGHAM, J. E., DARKE, A. H., REID, J. S. G. & GIDLEY, M. J. 1998. Structural aspects of the interaction of mannan-based polysaccharides with bacterial cellulose. <i>Carbohydrate Research</i>, 307, 299309. XIONG, G., CHENG, K. & PAULY, M. Xylan O-Acetylation Impacts Xylem Development and Enzymatic Recalcitrance as Indicated by the Arabidopsis Mutant tbl29. <i>Molecular Plant</i>, 6, 1373-1375. YU, L., LYCZAKOWSKI, J. J., PEREIRA, C. S., KOTAKE, T., YU, X., LI, A., MOGELSVANG, S., SKAF, M. S. & DUPREE, P. 2018. The patterned structure of galactoglucomannan suggests it may bind to cellulose in seed mucilage. <i>Plant Physiology</i>, 178, 1011-1026. ZHANG, T., ZHENG, Y. Z. & COSGROVE, D. J. 2016. Spatial organization of cellulose microfibrils and matrix polysaccharides in primary plant cell walls as imaged by multichannel atomic force microscopy. <i>Plant Journal</i>, 85, 179-192. ZHANG, X. Y., DOMINGUEZ, P. G., KUMAR, M., BYGDELL, J., MIROSHNICHENKO, S., SUNDBERG, B., WINGSLE, G. & NIITTYLA, T. 2018. Cellulose Synthase Stoichiometry in Aspen Differs from Arabidopsis 		
 1998. Structural aspects of the interaction of mannan-based polysaccharides with bacterial cellulose. <i>Carbohydrate Research</i>, 307, 299309. XIONG, G., CHENG, K. & PAULY, M. Xylan O-Acetylation Impacts Xylem Development and Enzymatic Recalcitrance as Indicated by the Arabidopsis Mutant tbl29. <i>Molecular Plant</i>, 6, 1373-1375. YU, L., LYCZAKOWSKI, J. J., PEREIRA, C. S., KOTAKE, T., YU, X., LI, A., MOGELSVANG, S., SKAF, M. S. & DUPREE, P. 2018. The patterned structure of galactoglucomannan suggests it may bind to cellulose in seed mucilage. <i>Plant Physiology</i>, 178, 1011-1026. ZHANG, T., ZHENG, Y. Z. & COSGROVE, D. J. 2016. Spatial organization of cellulose microfibrils and matrix polysaccharides in primary plant cell walls as imaged by multichannel atomic force microscopy. <i>Plant Journal</i>, 85, 179-192. ZHANG, X. Y., DOMINGUEZ, P. G., KUMAR, M., BYGDELL, J., MIROSHNICHENKO, S., SUNDBERG, B., WINGSLE, G. & NIITTYLA, T. 2018. Cellulose Synthase Stoichiometry in Aspen Differs from Arabidopsis 		
 with bacterial cellulose. <i>Carbohydrate Research</i>, 307, 299309. XIONG, G., CHENG, K. & PAULY, M. Xylan O-Acetylation Impacts Xylem Development and Enzymatic Recalcitrance as Indicated by the Arabidopsis Mutant tbl29. <i>Molecular Plant</i>, 6, 1373-1375. YU, L., LYCZAKOWSKI, J. J., PEREIRA, C. S., KOTAKE, T., YU, X., LI, A., MOGELSVANG, S., SKAF, M. S. & DUPREE, P. 2018. The patterned structure of galactoglucomannan suggests it may bind to cellulose in seed mucilage. <i>Plant Physiology</i>, 178, 1011-1026. ZHANG, T., ZHENG, Y. Z. & COSGROVE, D. J. 2016. Spatial organization of cellulose microfibrils and matrix polysaccharides in primary plant cell walls as imaged by multichannel atomic force microscopy. <i>Plant Journal</i>, 85, 179-192. ZHANG, X. Y., DOMINGUEZ, P. G., KUMAR, M., BYGDELL, J., MIROSHNICHENKO, S., SUNDBERG, B., WINGSLE, G. & NIITTYLA, T. 2018. Cellulose Synthase Stoichiometry in Aspen Differs from Arabidopsis 		
 XIONG, G., CHENG, K. & PAULY, M. Xylan O-Acetylation Impacts Xylem Development and Enzymatic Recalcitrance as Indicated by the Arabidopsis Mutant tbl29. <i>Molecular Plant</i>, 6, 1373-1375. YU, L., LYCZAKOWSKI, J. J., PEREIRA, C. S., KOTAKE, T., YU, X., LI, A., MOGELSVANG, S., SKAF, M. S. & DUPREE, P. 2018. The patterned structure of galactoglucomannan suggests it may bind to cellulose in seed mucilage. <i>Plant Physiology</i>, 178, 1011-1026. ZHANG, T., ZHENG, Y. Z. & COSGROVE, D. J. 2016. Spatial organization of cellulose microfibrils and matrix polysaccharides in primary plant cell walls as imaged by multichannel atomic force microscopy. <i>Plant Journal</i>, 85, 179-192. ZHANG, X. Y., DOMINGUEZ, P. G., KUMAR, M., BYGDELL, J., MIROSHNICHENKO, S., SUNDBERG, B., WINGSLE, G. & NIITTYLA, T. 2018. Cellulose Synthase Stoichiometry in Aspen Differs from Arabidopsis 		· · · · · · · · · · · · · · · · · · ·
 Bevelopment and Enzymatic Recalcitrance as Indicated by the Arabidopsis Mutant tbl29. <i>Molecular Plant</i>, 6, 1373-1375. YU, L., LYCZAKOWSKI, J. J., PEREIRA, C. S., KOTAKE, T., YU, X., LI, A., MOGELSVANG, S., SKAF, M. S. & DUPREE, P. 2018. The patterned structure of galactoglucomannan suggests it may bind to cellulose in seed mucilage. <i>Plant Physiology</i>, 178, 1011-1026. ZHANG, T., ZHENG, Y. Z. & COSGROVE, D. J. 2016. Spatial organization of cellulose microfibrils and matrix polysaccharides in primary plant cell walls as imaged by multichannel atomic force microscopy. <i>Plant Journal</i>, 85, 179-192. ZHANG, X. Y., DOMINGUEZ, P. G., KUMAR, M., BYGDELL, J., MIROSHNICHENKO, S., SUNDBERG, B., WINGSLE, G. & NIITTYLA, T. 2018. Cellulose Synthase Stoichiometry in Aspen Differs from Arabidopsis 		
 Mutant tbl29. <i>Molecular Plant</i>, 6, 1373-1375. YU, L., LYCZAKOWSKI, J. J., PEREIRA, C. S., KOTAKE, T., YU, X., LI, A., MOGELSVANG, S., SKAF, M. S. & DUPREE, P. 2018. The patterned structure of galactoglucomannan suggests it may bind to cellulose in seed mucilage. <i>Plant Physiology</i>, 178, 1011-1026. ZHANG, T., ZHENG, Y. Z. & COSGROVE, D. J. 2016. Spatial organization of cellulose microfibrils and matrix polysaccharides in primary plant cell walls as imaged by multichannel atomic force microscopy. <i>Plant Journal</i>, 85, 179-192. ZHANG, X. Y., DOMINGUEZ, P. G., KUMAR, M., BYGDELL, J., MIROSHNICHENKO, S., SUNDBERG, B., WINGSLE, G. & NIITTYLA, T. 2018. Cellulose Synthase Stoichiometry in Aspen Differs from Arabidopsis 		
 YU, L., LYCZAKOWSKI, J. J., PEREIRA, C. S., KOTAKE, T., YU, X., LI, A., MOGELSVANG, S., SKAF, M. S. & DUPREE, P. 2018. The patterned structure of galactoglucomannan suggests it may bind to cellulose in seed mucilage. <i>Plant Physiology,</i> 178, 1011-1026. ZHANG, T., ZHENG, Y. Z. & COSGROVE, D. J. 2016. Spatial organization of cellulose microfibrils and matrix polysaccharides in primary plant cell walls as imaged by multichannel atomic force microscopy. <i>Plant Journal,</i> 85, 179-192. ZHANG, X. Y., DOMINGUEZ, P. G., KUMAR, M., BYGDELL, J., MIROSHNICHENKO, S., SUNDBERG, B., WINGSLE, G. & NIITTYLA, T. 2018. Cellulose Synthase Stoichiometry in Aspen Differs from Arabidopsis 		
 MOGELSVANG, S., SKAF, M. S. & DUPREE, P. 2018. The patterned structure of galactoglucomannan suggests it may bind to cellulose in seed mucilage. <i>Plant Physiology</i>, 178, 1011-1026. ZHANG, T., ZHENG, Y. Z. & COSGROVE, D. J. 2016. Spatial organization of cellulose microfibrils and matrix polysaccharides in primary plant cell walls as imaged by multichannel atomic force microscopy. <i>Plant Journal</i>, 85, 179-192. ZHANG, X. Y., DOMINGUEZ, P. G., KUMAR, M., BYGDELL, J., MIROSHNICHENKO, S., SUNDBERG, B., WINGSLE, G. & NIITTYLA, T. 2018. Cellulose Synthase Stoichiometry in Aspen Differs from Arabidopsis 		
 structure of galactoglucomannan suggests it may bind to cellulose in seed mucilage. <i>Plant Physiology</i>, 178, 1011-1026. ZHANG, T., ZHENG, Y. Z. & COSGROVE, D. J. 2016. Spatial organization of cellulose microfibrils and matrix polysaccharides in primary plant cell walls as imaged by multichannel atomic force microscopy. <i>Plant Journal</i>, 85, 179-192. ZHANG, X. Y., DOMINGUEZ, P. G., KUMAR, M., BYGDELL, J., MIROSHNICHENKO, S., SUNDBERG, B., WINGSLE, G. & NIITTYLA, T. 2018. Cellulose Synthase Stoichiometry in Aspen Differs from Arabidopsis 		
 mucilage. <i>Plant Physiology</i>, 178, 1011-1026. ZHANG, T., ZHENG, Y. Z. & COSGROVE, D. J. 2016. Spatial organization of cellulose microfibrils and matrix polysaccharides in primary plant cell walls as imaged by multichannel atomic force microscopy. <i>Plant Journal</i>, 85, 179-192. ZHANG, X. Y., DOMINGUEZ, P. G., KUMAR, M., BYGDELL, J., MIROSHNICHENKO, S., SUNDBERG, B., WINGSLE, G. & NIITTYLA, T. 2018. Cellulose Synthase Stoichiometry in Aspen Differs from Arabidopsis 		
 ZHANG, T., ZHENG, Y. Z. & COSGROVE, D. J. 2016. Spatial organization of cellulose microfibrils and matrix polysaccharides in primary plant cell walls as imaged by multichannel atomic force microscopy. <i>Plant Journal</i>, 85, 179-192. ZHANG, X. Y., DOMINGUEZ, P. G., KUMAR, M., BYGDELL, J., MIROSHNICHENKO, S., SUNDBERG, B., WINGSLE, G. & NIITTYLA, T. 2018. Cellulose Synthase Stoichiometry in Aspen Differs from Arabidopsis 		
 cellulose microfibrils and matrix polysaccharides in primary plant cell walls as imaged by multichannel atomic force microscopy. <i>Plant Journal</i>, 85, 179-192. ZHANG, X. Y., DOMINGUEZ, P. G., KUMAR, M., BYGDELL, J., MIROSHNICHENKO, S., SUNDBERG, B., WINGSLE, G. & NIITTYLA, T. 2018. Cellulose Synthase Stoichiometry in Aspen Differs from Arabidopsis 		5 F 6F
 imaged by multichannel atomic force microscopy. <i>Plant Journal</i>, 85, 179-192. ZHANG, X. Y., DOMINGUEZ, P. G., KUMAR, M., BYGDELL, J., MIROSHNICHENKO, S., SUNDBERG, B., WINGSLE, G. & NIITTYLA, T. 2018. Cellulose Synthase Stoichiometry in Aspen Differs from Arabidopsis 		
 ZHANG, X. Y., DOMINGUEZ, P. G., KUMAR, M., BYGDELL, J., MIROSHNICHENKO, S., SUNDBERG, B., WINGSLE, G. & NIITTYLA, T. 2018. Cellulose Synthase Stoichiometry in Aspen Differs from Arabidopsis 		
 MIROSHNICHENKO, S., SUNDBERG, B., WINGSLE, G. & NIITTYLA, T. 2018. Cellulose Synthase Stoichiometry in Aspen Differs from Arabidopsis 		
2018. Cellulose Synthase Stoichiometry in Aspen Differs from Arabidopsis		
and Norway Spruce. Plant Physiology, 177, 1096-1107.		
	82/	and Norway Spruce. Flanc Flyslology, 111, 1090-1101.

859 Figure legends

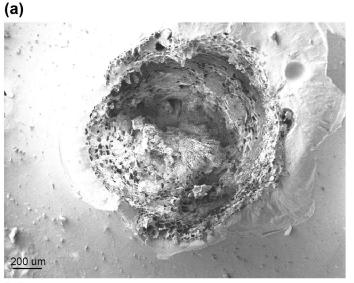
Figure 1. cryo-SEM analysis of spruce stem sections. (a) to (f) Representative images of stem sections of one-year-old spruce branch at different magnifications. Red arrows indicate tracheids (b), macrofibril bundles (c and d) and individual macrofibrils (e and f). Scale bars are provided for each image.

Figure 2. cryo-SEM analysis of poplar stem sections (a) to (e) Representative 864 images of stem sections of *in vitro* grown poplar trees at different magnifications. Red 865 arrows show vessels (b) and macrofibrils (c and e). Yellow arrows indicate fibre cells 866 (b). Higher magnification images (c, d and e) are presented for vessels. Scale bars 867 are provided for each image. (f) Diameter of spruce tracheid cell wall fibrils compared 868 to these observed in poplar vessel cell walls. For each bar 150 individual fibrils were 869 measured. Boxplots mark the median and show between 25th and 75th percentile of 870 the data. *** denotes $p \le 0.00001$ in Student's t-test. 871

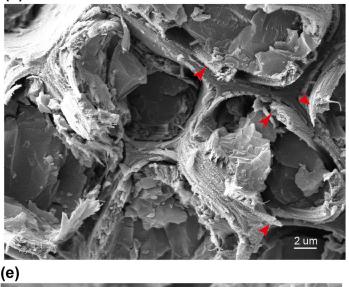
Figure 3. Analysis of Arabidopsis stem sections and fibrous cellulose. (a) to (c) Imaging of WT vessels at increasing magnification (d) Imaging of fibrous cellulose standard from cotton linters shows cell wall fibrils with an appearance similar to structures seen *in planta*. (e) Imaging of individual vessels in WT plants. (f) Imaging of individual vessels in *irx3* plants. (g) and (f) Macrofibrils are detectable in WT Arabidopsis and are absent in *irx3* secondary cell walls. Red arrows indicate the macrofibril structures throughout the figure. Scale bars are provided for each image.

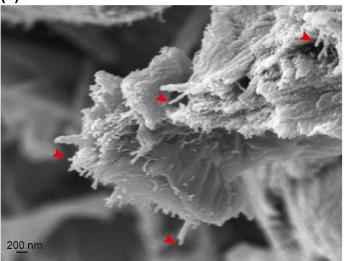
Figure 4. Analysis of macrofibrils in mutant Arabidopsis plants. Representative image of (a) *irx9*, (b) *irx10*, (c) *esk1*, (d) *4cl1*, (e) *lac4* and (f) *csla2/3/9* Arabidopsis macrofibrils. Scale bar corresponds to 200 nm on each image. (g) Quantification of macrofibril diameter in WT and mutant Arabidopsis plants. N = 150. Boxplots mark a median and show between 25th and 75th percentile of the data. *** denotes p \leq

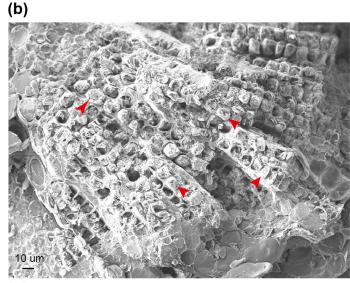
884 0.00001, ** denotes $p \le 0.0001$, * denotes $p \le 0.05$ in Tukey test following ANOVA 885 when compared to WT, ns indicates lack of statistically significant difference.



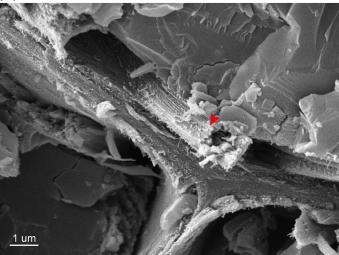
(c)

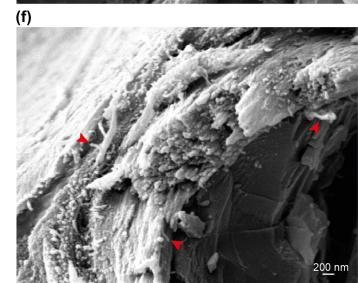


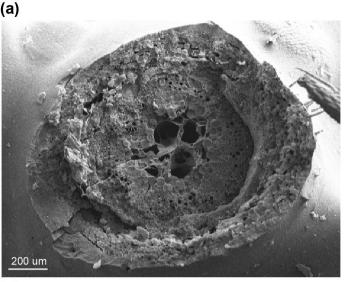


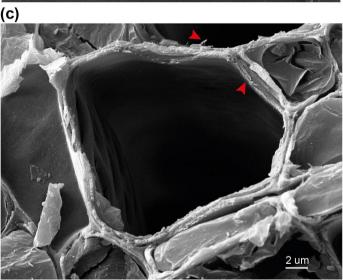


(d)

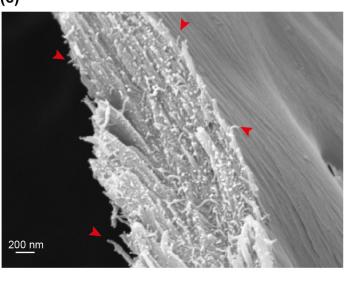


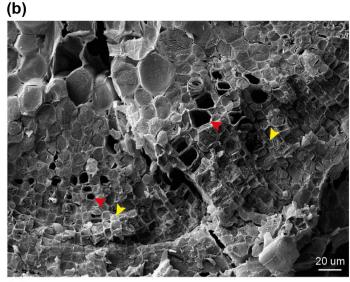




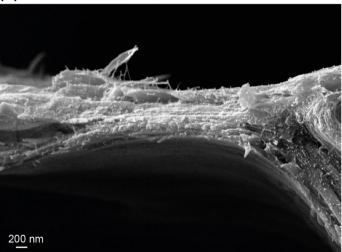


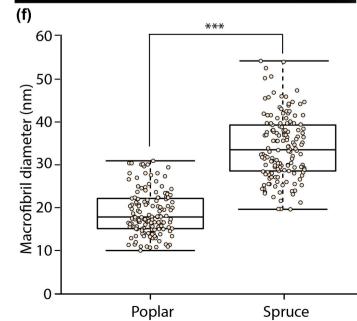
(e)





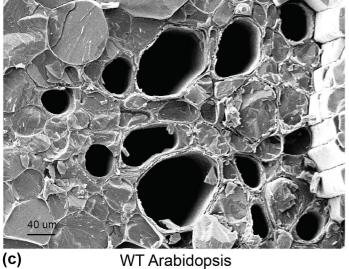
(d)



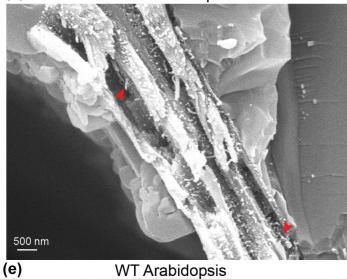


(a)

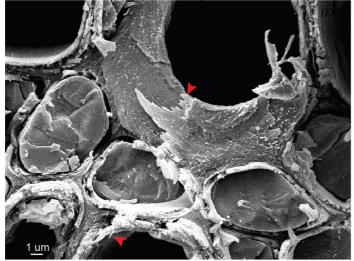
WT Arabidopsis available under a CC-BY-NC-ND(40) International license. WT Arabidopsis



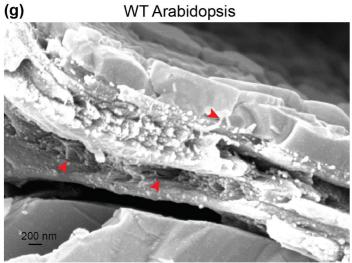
WT Arabidopsis

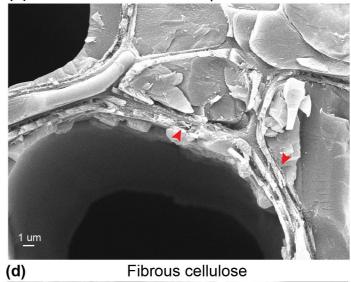


WT Arabidopsis



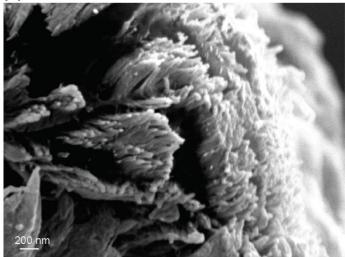
WT Arabidopsis



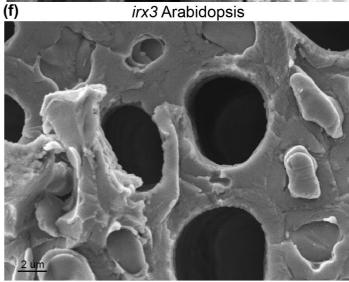




Fibrous cellulose



irx3 Arabidopsis



irx3 Arabidopsis



